ARL-TR-7464 ● SEP 2015

US Army Research Laboratory

Gas Control and Thermal Modeling Methods for Pressed Pellet and Fast Rise Thin-Film Thermal Batteries

by Frank C Krieger and Michael S Ding

NOTICES

Disclaimers

The findings in this report are not to be construed as an official Department of the Army position unless so designated by other authorized documents.

Citation of manufacturer's or trade names does not constitute an official endorsement or approval of the use thereof.

Destroy this report when it is no longer needed. Do not return it to the originator.

ARL-TR-7464 ● SEP 2015

US Army Research Laboratory

Gas Control and Thermal Modeling Methods for Pressed Pellet and Fast Rise Thin-Film Thermal Batteries

by Frank C Krieger and Michael S Ding
Sensors and Electron Devices Directorate, ARL

REPORT DOCUMENTATION PAGE	Form Approved OMB No. 0704-0188

1. REPORT DATE *(DD-MM-YYYY)*	2. REPORT TYPE	3. DATES COVERED (From - To)
Sep 2015	Final	10/2014 to 09/2015

4. TITLE AND SUBTITLE	5a. CONTRACT NUMBER
Gas Control and Thermal Modeling Methods for Pressed Pellet and Fast Rise Thin-Film Thermal Batteries	5b. GRANT NUMBER
	5c. PROGRAM ELEMENT NUMBER

6. AUTHOR(S)	5d. PROJECT NUMBER
Frank C Krieger and Michael S Ding	5e. TASK NUMBER
	5f. WORK UNIT NUMBER

7. PERFORMING ORGANIZATION NAME(S) AND ADDRESS(ES)	8. PERFORMING ORGANIZATION REPORT NUMBER
US Army Research Laboratory ATTN: RDRL-SED-C 2800 Powder Mill Road Adelphi, MD 20783-1138	ARL-TR-7464

9. SPONSORING/MONITORING AGENCY NAME(S) AND ADDRESS(ES)	10. SPONSOR/MONITOR'S ACRONYM(S)
	11. SPONSOR/MONITOR'S REPORT NUMBER(S)

12. DISTRIBUTION/AVAILABILITY STATEMENT

Approved for public release; distribution unlimited.

13. SUPPLEMENTARY NOTES

14. ABSTRACT

Pressed pellet thermal battery designs constitute the bulk of the present thermal battery industry. Thin-film fast rise thermal batteries are not yet in production, but are anticipated to supply important future niche applications in small-caliber arms and bunker penetrating munitions. Both types of thermal batteries can benefit significantly from improved gas control methods, thermal modeling, and design of experiment (DOE) statistical mathematical modeling analyses. Recent gas evolution experiments and analyses with operating pressed pellet thermal batteries are compared and discussed. Sierra Thermally Activated Battery Simulator (TABS) finite element models and US Army Research Laboratory (ARL) Fortran thermal battery mathematical optimization methods are described and illustrated for presently fielded thermal batteries and for the proposed new fast rise thin-film thermal batteries. Sierra TABS finite element thermal models can also be used with DOE statistical techniques to define and clarify electrochemical and thermodynamic relationships that occur within the thermal cell stacks during battery operation and that might be used to further enhance thermal battery operation. Proposed test fixtures and methods for significantly increasing the testing rates and relevant information quantities obtained from pressed pellet thermal battery gas evolution tests are shown and discussed.

15. SUBJECT TERMS

Thermal Battery, Thermal Modeling, Heat Transfer, Gas Control

16. SECURITY CLASSIFICATION OF:			17. LIMITATION OF ABSTRACT	18. NUMBER OF PAGES	19a. NAME OF RESPONSIBLE PERSON
a. REPORT	b. ABSTRACT	c. THIS PAGE			Frank C Krieger
Unclassified	Unclassified	Unclassified	UU	52	19b. TELEPHONE NUMBER (Include area code) 301-394-3115

Contents

List of Figures

Acknowledgments

We would like to acknowledge Ed Piekos and Anne Grillet of the Sandia National Laboratories in Albuquerque, New Mexico, who provided knowledgeable assistance and support on the Sierra Thermally Activated Battery Simulator (TABS) finite element models.

INTENTIONALLY LEFT BLANK.

1. Introduction

Pressed pellet thermal battery designs constitute the bulk of the present thermal battery industry.[1–5] Thin-film fast rise thermal batteries are not yet in production, but are anticipated to supply important future niche applications in small-caliber arms and bunker penetrating munitions.[6–8] Both types of thermal batteries can benefit significantly from improved gas control methods, thermal modeling, and design of experiment (DOE) statistical mathematical modeling analyses.[9–11]

The absence of hydrogen (H_2) gas in pressed pellet thermal battery operating atmospheres would permit the use of smaller munitions thermal batteries in the field as well as the more extensive use of economical non-micro-porous thermal insulators. Thermal modeling, when combined with experimental gas evolution tests of operating pressed pellet thermal batteries, clearly shows that H_2 gas removal has the potential to improve present pressed pellet munitions thermal reserve battery lifetimes by factors of 1.5 to 3 or more even when using expensive baseline micro-porous thermal insulators that show low baseline thermal conductivity values in H_2 gas atmospheres. Thermal lifetimes of pressed pellet thermal batteries that presently use economical non-micro-porous thermal insulators show much higher measured baseline thermal conductivity values in H_2 gas atmospheres and might be improved by factors of 5 or more with the removal of H_2 gas. H_2 gas removal methods from operating thermal batteries that are proposed in this report are simple, experimentally proven in previously reported gas evolution tests with commonly used thermal battery materials[3,4] and should be easily applicable to operating pressed pellet thermal batteries.

Recently measured evolved gas samples from operating thermal batteries are analyzed and compared with previous evolved gas measurements. Results from US Army Research Laboratory (ARL) Fortran and Sierra Thermally Activated Battery Simulator (TABS) finite element mathematical thermal battery optimization methods using representative operating thermal battery gas atmosphere compositions and pressures as input parameters for presently fielded pressed pellet thermal batteries as well as for potentially useful fast rise thin-film thermal battery applications are illustrated and discussed. Present Sierra TABS finite element models and ARL Fortran programs may be used in straightforward manners to calculate thermal battery lifetimes accurately from gross heat transfer considerations. Temperature changes within the operating cell stacks, however, are generally smaller than those used for gross heat transfer from the cell stack, have more complex origins, and are more difficult to measure experimentally. These smaller temperature changes and effects can be studied using a combination of experimental and DOE statistical methods. Such studies could be used to identify

electrochemical and thermodynamic processes that occur during battery operation (such as thermal cell heat generation) that could have great potential to improve thermal battery operation.[9–11]

Possible methods of accomplishing or improving present gas evolution testing procedures for previously manufactured thermal batteries already sealed into munitions or in storage are discussed briefly. Past efforts to evaluate methods of gas control on operating laboratory type thermal batteries have been hampered by the unacceptable amounts of time and effort required to build sufficient numbers of complete thermal batteries for testing.[5] This report therefore describes the construction and use of a simplified reusable thermal battery test fixture that permits rapid and comprehensive testing of selected thermal battery parameters under well-specified battery operating conditions.

The removal of H_2 gas from thermal battery atmospheres is only an important first step to increasing the lifetimes and energy densities of presently fielded production thermal batteries. Previously measured thermal battery performances, when analyzed using mathematical modeling methods, clearly show that enhanced gas control, combined with electrochemical and thermal optimization of thermal cell stacks and thermal battery insulation packages, will retain significant potential to improve thermal battery lifetimes and energy densities even after all H_2 gas has been removed.[1–11]

2. Pressed Pellet Thermal Battery Operating Gas Atmospheres and Gas Interactions

In this report, gas collection, measurement, and control methods for pyrotechnically heated thermal battery materials and operating thermal battery atmospheres are discussed with special emphasis on the removal of high thermal conductivity H_2 gas from pressed pellet thermal battery gas atmospheres by chemical oxidation to water (H_2O). Materials selection and chemical processing methods can and should be used to minimize the amount of chemically bound H_2 and H_2O originally present in the batteries after battery manufacture. The guaranteed absence of chemically bonded H_2, (typically dissolved in materials such as pyrotechnic iron and zirconium [Zr] particles) and of H_2O (typically present in the hygroscopic electrolytes, adsorbed onto the porous thermal insulation, and possibly reintroduced in small amounts during battery construction) from fully assembled thermal batteries by materials choices and chemical processing methods alone seems difficult. Some method of removing at least some small amount of H_2 after battery initiation seems necessary.

When H_2 gas is oxidized to H_2O, some form (either simple or complex and indirect) of the cyclic reaction between water, oxygen, and hydrogen ($2H_2O \leftrightarrow 2H_2 + O_2$) might be expected in both stored and operating thermal batteries, and such reactions must be avoided. The complexity and chemical reactivity of thermal battery chemical compounds, the long required shelf lives (typically, 20 to 40 years), the high operational temperatures (pyrotechnic temperatures may reach ~1500 °C during battery activation), and the wide range of sometimes rapidly changing temperatures experienced both during battery storage and operation limits methods of H_2 removal that exclude the possibility of circumstances arising that permit H_2 formation from the chemical reaction $2H_2O \leftrightarrow 2H_2 + O_2$ both before and during thermal battery operation. It should be noted here that any H_2 generated during battery storage could be effectively removed by the same method used for removal of the presumably much larger quantity of H_2 generated on battery activation.

One method of permanently removing H_2 gas by chemical oxidation proven in gas evolution tests of thermal battery materials is to expose the H_2 gas to heated mixtures of Zr/barium chromate ($BaCrO_4$) pyrotechnic powder mixtures with low Zr percentages (~22/78 Zr/$BaCrO_4$ wt %). Water formed from the resulting H_2 oxidation appears to react with the pyrotechnic ash to remove H_2 while forming oxides that remain chemically bonded to the ash. With high Zr heat powder weight percentages near the stoichiometric ratio (~28/72 Zr/$BaCrO_4$), large amounts of H_2 gas are typically formed on pyrotechnic initiation. Pyrotechnically heated mixtures of ~28/72 wt % Zr/$BaCrO_4$ heat powder paper with extra $BaCrO_4$ powder in physical contact showed that the ash from ignition of the resulting mixture could remove nearly all of the H_2 gas evolved from the ignition of the heat paper.[3,4] Similar pyrotechnically heated mixtures of ~22/78 wt % Zr/$BaCrO_4$ heat powder plus additional $BaCrO_4$ powder should be effective in removing high thermal conductivity H_2 gas from operating thermal battery atmospheres. Actual removal of H_2 gas in the operating thermal battery described below, however, appeared to be severely limited, possibly by the significant quantities of carbon monoxide (CO) and carbon dioxide (CO_2) gases in the thermal battery operating atmosphere. Significant reduction of evolved CO and CO_2 gas quantities in thermal battery atmospheres could be achieved by reducing or eliminating the amounts of organic binder materials in thermal battery insulation packages.

3. Experimental

Thermal batteries built into thin-wall stainless steel (SS) thermal battery cases with hermetic gas handling fittings attached were coupled to a hermetically sealed gas handling system (GHS), after which the entire system including the thermal battery internal components (void volume) was evacuated to a nominal fore pump vacuum

pressure of ~50 microns of mercury. The interconnected thermal battery-GHS system was then sealed, the thermal battery was initiated, and the evolved gas volumes, temperatures, and compositions were measured. The resulting gas pressures and temperatures during and after thermal battery electrical operation were recorded using an Agilent 34970A Data Acquisition/Switch Unit with MKS Baratron dual capacitance manometer pressure transducers and a nominal sampling rate of 10 samples/s. Gas compositions were analyzed using an Agilent 7890A gas chromatograph (GC) with a 50-µl sample loop and a thermal conductivity detector.[1–5] The GC column used to measure the gas compositions was a Carboxen 1010 fused silica chromatographic porous layer open tubular (PLOT) capillary column (30 m long x 0.32 mm diameter x 15 µm average film thickness) with a maximum isothermal operating temperature of 250 °C. The sample gases for the GC calibration were certified by the supplier as being accurate to 2.95% for each individual sample gas amount present. The calculated accuracy of the gas compositions reported is generally within ±10% of the value actually measured, which means that if a gas is reported as comprising 10% of a mixture, then the actual percentage of that gas in that mixture will be somewhere between 9% and 11%. Ultra-high purity (UHP) grade argon was the carrier gas used for the GC.

The GHS, the 10-cc internal volume SS gas collection cylinders, and the battery void volumes were flushed with chemically inert gases (helium or argon) or with dry room air, as appropriate, using a fore pump capable of supplying a minimum pressure of approximately 5 x 10^{-2} torr (6.7 Pa). All of the gas and GHS volumes were measured relative to the internal volume of a 10-cc SS sample bottle, using the ideal gas law. The 10-cc SS sample bottle internal volume was accurate to ±10%. Absolute gas volumes were therefore measured to an accuracy of approximately ±10%. Relative gas volumes, however, and gas volumes relative to the 10-cc internal volume SS sample bottle, were measured to a precision of better than ±0.1% using the dual capacitance manometers. Global measured leak rates of the entire evacuated GHS were measured by pressure readings taken over periods of several days or weeks and ranged from 5.3 E–5 to 6.3 E–6 std-atm-cc/s. The batteries were tested in a temperature equilibrated Tenney temperature chamber at –40 °C and remained in the operating Tenney chamber with the chamber temperature holding at –40 °C throughout the tests. Additional experimental and calculation methods have been described previously.[1–5]

The first gas sample bottle was attached to the GHS-battery void volume coupled system, and the entire system was evacuated to a fore pump gas pressure of nominally 50 microns of mercury. The entire system was then sealed by closing the valve to the fore pump. The sample bottle remained open when the battery was initiated and was closed nominally 15 s after pyrotechnic initiation. Sample bottle

opening times after the first sample bottle were recorded manually for confirmation purposes, but were then referenced to the initial pressure drops of the curves shown in Figs. 7 and 8. Reported times for opening the individual sample bottles referenced from the moment of initial gas pressure rise in the GHS are therefore digitally confirmable to an accuracy of nominally 0.1 s except for the first sample bottle.

The collected and measured gases were hydrogen, oxygen, nitrogen, carbon monoxide, methane, and carbon dioxide (H_2, O_2, N_2, CO, CH_4, and CO_2). These 6 gases have previously been shown to constitute more than 94% of the total gases present in operating thermal batteries exclusive of any H_2O that might be formed. H_2O is known to be evolved in operating thermal batteries based on previous gas evolution tests, but cannot ordinarily be measured accurately in operating batteries because H_2O may adsorb onto the porous thermal insulation or other test system components, and because many of the thermal battery chemical components are hygroscopic. The low ambient temperatures (–40 °C) of the batteries tested in this report would have made meaningful water determinations during battery operation additionally difficult.

4. Measured Compositions and Volumes of Gases Evolved from Operating Thermal Batteries

Measured evolved gas mixture compositions from hermetically sealed thermal batteries tested with and without adding ~22/78 wt % Zr/$BaCrO_4$ heat paper powder mixed with additional $BaCrO_4$ powder and placed into the thermal insulation package to remove H_2 gas are shown below (Figs. 1–6). Before the tests described below were done, some initial screening tests using thermal batteries of the same design were done based only on battery electrical performance in an attempt to rapidly determine an optimum weight ratio between the ~22/78 wt % Zr/$BaCrO_4$ heat paper powder and the added $BaCrO_4$ powder. For the screening tests based on electrical performance, gas evolution characteristics were not measured, and a direct relationship between electrical lifetime, H_2 gas evolution, and thermal cell stack cooling was assumed. All of the batteries tested, including the 2 batteries analyzed in detail for this report, performed normally and easily exceeded the required electrical output, as expected. Unfortunately, the batteries showed unexpectedly large inherent electrical performance variations, and the apparent ~60% electrical lifetime improvement originally observed from adding the ~22/78 wt % Zr/$BaCrO_4$ heat paper powder with additional $BaCrO_4$ powder to the battery insulation package evaluated on the basis of battery electrical performance screening tests only was not reproducible.

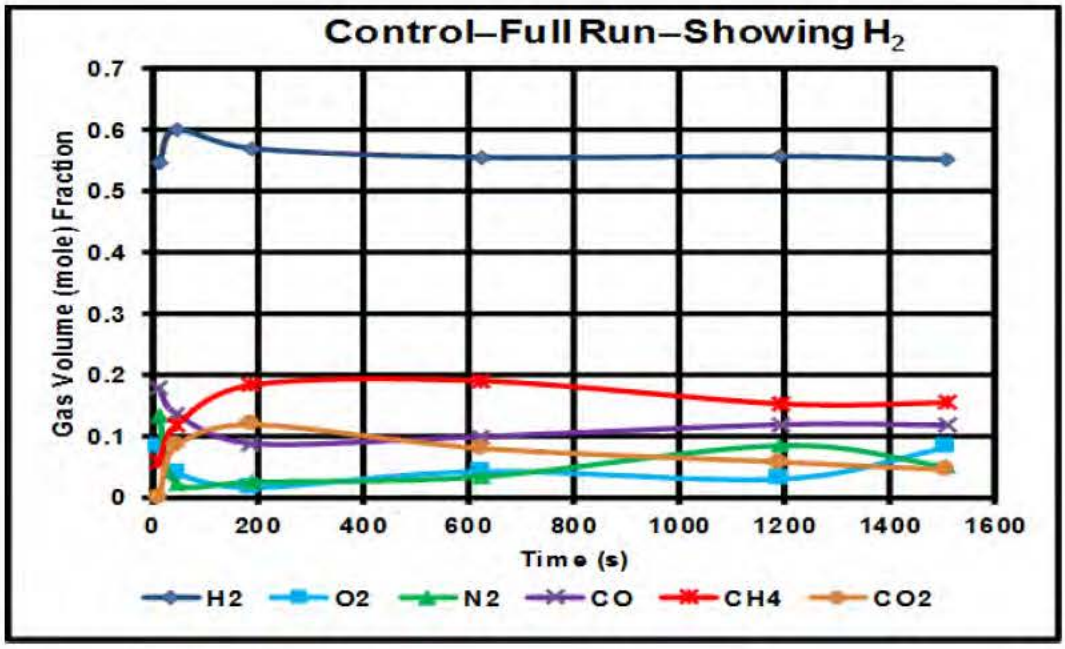

Fig. 1 Pressed pellet thermal battery operating gas atmosphere fractions – Control – Full Run – Showing H_2 – No Zr/$BaCrO_4$

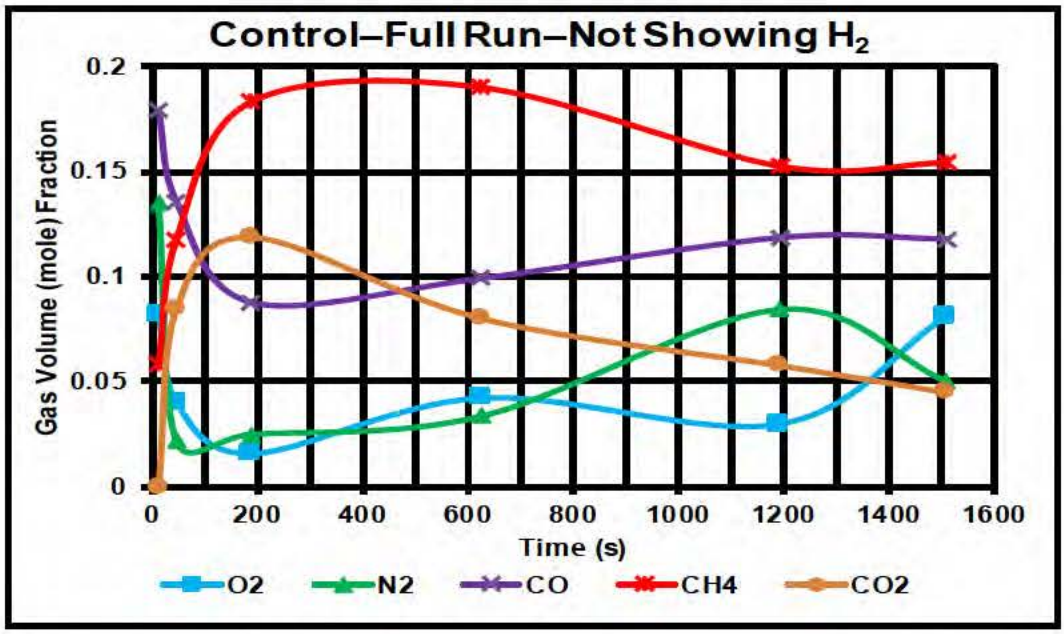

Fig. 2 Pressed pellet thermal battery operating gas atmosphere fractions – Control – Full Run – Not Showing H_2 – No Zr/$BaCrO_4$

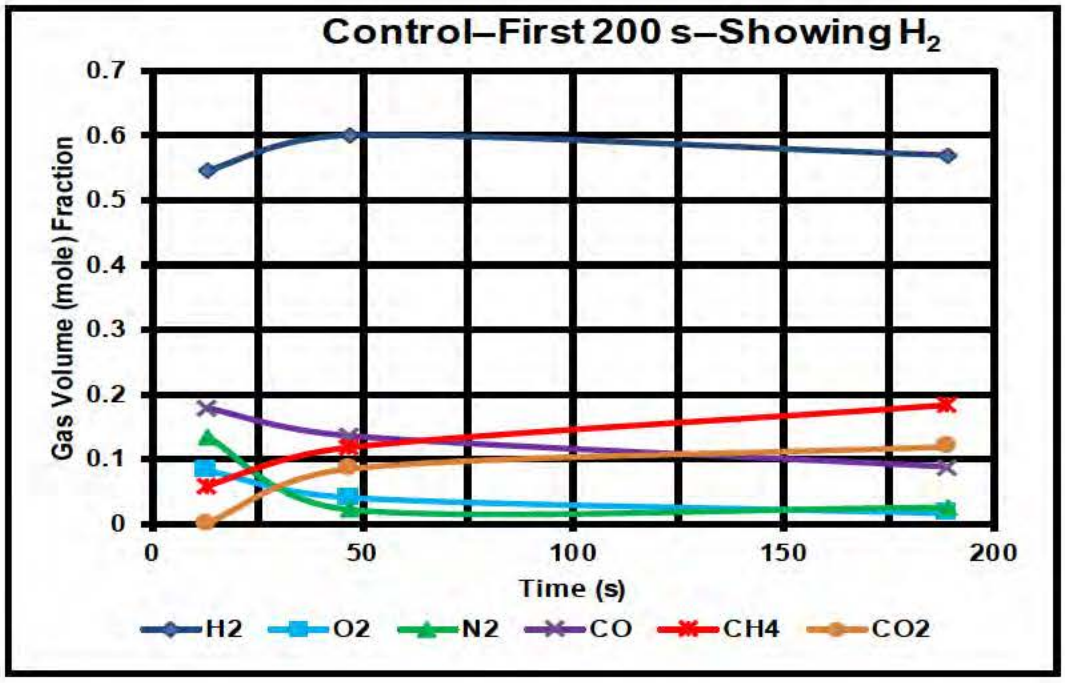

Fig. 3 Pressed pellet thermal battery operating gas atmosphere fractions – Control – First 200 s – Showing H_2 – No $Zr/BaCrO_4$

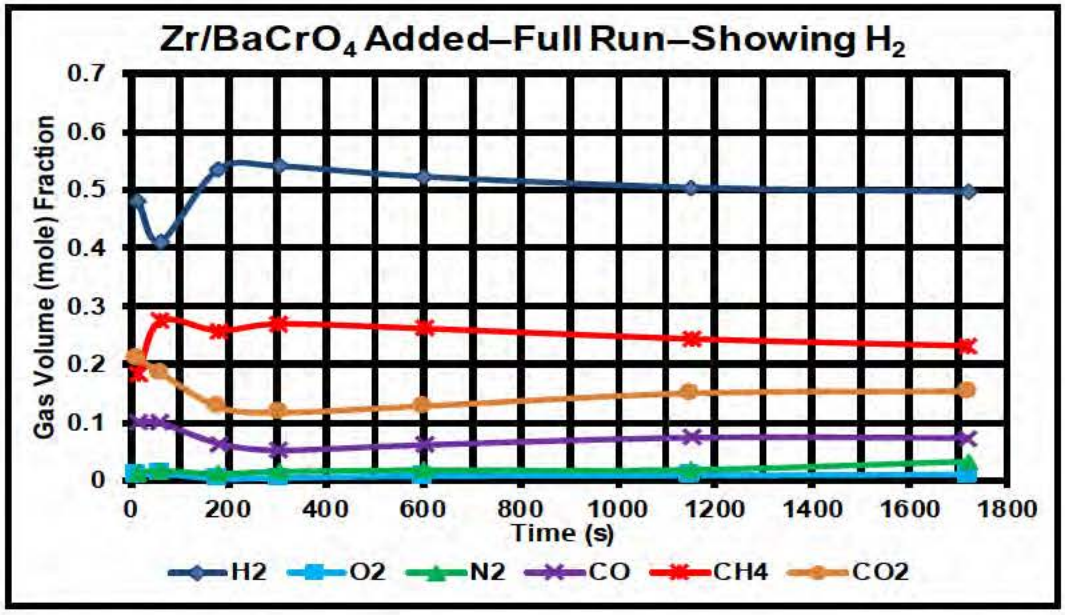

Fig. 4 Pressed pellet thermal battery operating gas atmosphere fractions – With Heated $Zr/BaCrO_4$ – Full Run – Showing H_2

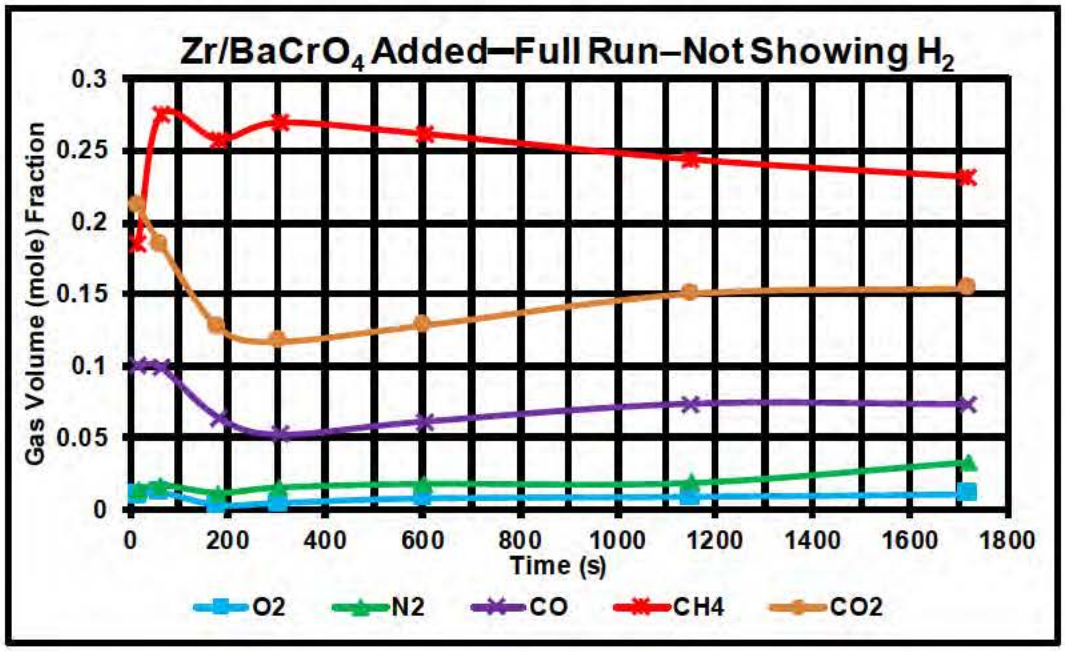

Fig. 5 Pressed pellet thermal battery operating gas atmosphere fractions – With Heated $Zr/BaCrO_4$ – Full Run – Not Showing H_2

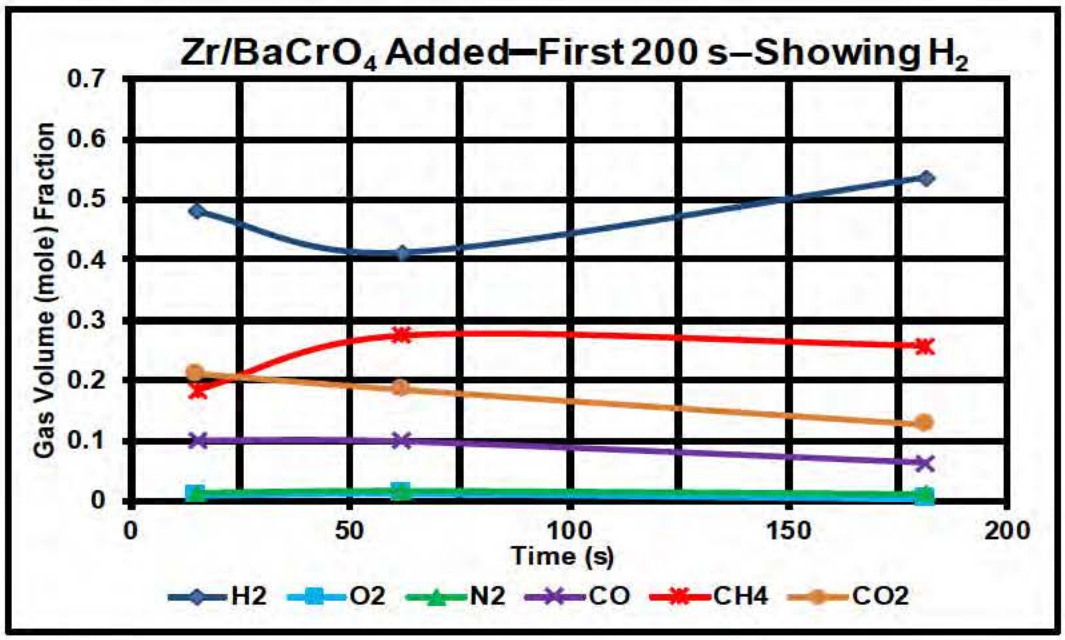

Fig. 6 Pressed pellet thermal battery operating gas atmosphere fractions – With Heated $Zr/BaCrO_4$ – First 200 s – Showing H_2

Based on the screening results from the batteries evaluated only by electrical performance, a $Zr/BaCrO_4$ mixture with a weight fraction (0.5751) of added $BaCrO_4$ (6.01 g $BaCrO_4$ and 4.44 g of ~22/78 wt % $Zr/BaCrO_4$ powder) was used in the operating battery test of this report. This compares with the 0.3113 weight

fraction of added $BaCrO_4$ that was used in the previous[3] more controlled gas evolution test that had removed 18.78 std-atm-cc of H_2 gas/g of added $BaCrO_4$ (1.0950 g added $BaCrO_4$ and 2.4224 g of ~28/72 wt % Zr/$BaCrO_4$ heat powder paper).

The H_2 gas removal capability of the oxidizing powder ash in the battery might have actually been decreased (or eliminated) rather than increased by adding the additional $BaCrO_4$ based on the battery screening tests either because of changes in the chemical composition of the ash or because the additional mass of the $BaCrO_4$ caused the resulting powder ash to be insufficiently heated. It should also be noted that the original experiment where 18.78 std-atm-cc of H_2 gas was removed per g of added $BaCrO_4$ used ~28/72 Zr/$BaCrO_4$ heat powder paper. That ~28/72 Zr/$BaCrO_4$ heat powder paper was ignited to produce the H_2 gas that was then removed with the added $BaCrO_4$. The ~28/72 Zr/$BaCrO_4$ heat powder paper with the added $BaCrO_4$ would have had an inherently higher peak temperature than the ~22/78 Zr/$BaCrO_4$ heat powder that was used in the present experiment. The ~22/78 Zr/$BaCrO_4$ heat powder was used in the present experiment because it has been proven not to evolve significant quantities of H_2 gas.[3,4] Proper pyrotechnic ash temperature maintenance and chemical composition are among the factors that should be more completely investigated in future experiments.

The baseline (control) battery test for this report did not use any added H_2 oxidizing powder. Both batteries analyzed in detail for this report were repackaged production thermal batteries with hermetically sealed cases specially designed for the collection of evolved gases. Both batteries used the same reduced current drain so that the electrochemistry could supply an electrical life ~3 times longer than normally required in anticipation of an improved electrical lifetime from better temperature control as a result of H_2 gas removal. Although all phases of both battery tests described below worked properly, the H_2 gas fraction in the battery with the pyrotechnically heated Zr/$BaCrO_4$ powders remained unacceptably high. The electrical lifetime and the H_2 gas fraction in the operating battery with the heated Zr/$BaCrO_4$ powder ash were both very similar to those of the baseline (control) battery where no attempt at all was made to remove H_2 (Figs. 1–6). For both batteries, evolved gas samples were taken at nominal times of 15, 60, 180, 600, 1200, and 1600 s after pyrotechnic initiation, and for both batteries the gas compositions measured for the first three gas samples are of particular interest.

The rapid initial rise of the CH_4 gas fraction combined with the relatively constant H_2 gas fraction in Figs. 1–6 strongly suggests that CH_4 formation cannot be resulting only from the H_2 gas present. If CH_4 were coming only from H_2 and no additional H_2 were being formed, the increase in the CH_4 volume fraction would be exactly half the reduction in the H_2 volume fraction. The H_2 volume fraction stays

relatively constant after 200 s, which suggests that the H_2 remains chemically inactive after the first 200 s. The chemical complexity of the gas and solid interactions that take place initially permits numerous inferences regarding the gas reactions, while examination of the measured gas data generally permits exclusion of many of those inferences.

The relative gas fractions formed during the first 200 s as well as those formed 24 or more hours after ignition were similar for most pressed pellet thermal batteries, but differed sufficiently (and sometimes substantially) so that those gas compositions could be used with additional experimental information to help confirm materials, internal heat balances, and chemical processing methods used in thermal battery construction.

Gas composition and volumetric analyses described below give some indication that ignition and thermal decomposition of the organic binder in the thermal insulation might have formed enough CO, CO_2, and H_2O to react with the heated Zr/$BaCrO_4$ powder ash significantly enough when the ~22/78 wt % Zr/$BaCrO_4$ heat powder with added $BaCrO_4$ was ignited in the presence of the thermal insulation with organic binders so that the heated Zr/$BaCrO_4$ ash mixture was then unable to react sufficiently with H_2 gas. The dip and recovery of the H_2 fraction in the operating gas atmosphere from 0 to 200 s for the battery with the heated Zr/$BaCrO_4$ ash in the thermal insulation (Figs. 4 and 6) shows that some H_2 removal did take place and also shows that competing chemical reactions are present. The very low fractions of O_2 and N_2 in the battery containing heated Zr/$BaCrO_4$ ash relative to the control battery suggest chemical reactions of those gases with the heated powder ash. Evolved CO and CO_2 gas quantities might be reduced or eliminated by reducing or eliminating the amount of organic material from the battery construction materials such as the thermal insulators and tapes. The thermal insulation with the organic binder believed to be responsible for most of the CO, CO_2, and H_2O gas evolution in these battery tests could easily be replaced with a thermal insulation made from inorganic binder materials with nearly identical thermal properties that would not outgas significantly at high temperatures.

All of the gas evolution tests of this report, along with most previous gas evolution tests of thermal batteries and thermal battery materials, produced initial gas compositions within the first 200 s of pyrotechnic initiation that subsequently changed only slowly throughout the remainder of the test. In previously reported materials gas evolution tests for individual materials, both ~22/78 wt % Zr/$BaCrO_4$ heat powder (low total gas volumes) and ~28/72 wt % Zr/$BaCrO_4$ heat powder paper (high total gas volumes) behaved in this manner and both evolved nominally 0.80 volume (mole) fraction H_2 gas when tested individually.[3,4] The gas mixture standard temperature and pressure (STP) volumes typically increase substantially

at relatively constant rates during the first ~200 s after pyrotechnic initiation and then decrease slowly.

For both battery tests, the GHS remained open to the battery throughout the test so the effect of changes in the gas composition occurring within the battery voids might have been masked to some extent by inhibited mixing between the changing gas compositions present in the battery void volumes with the gas compositions already present in the GHS. As is shown in the gas volume calculations below, however, the internal volume of the GHS is similar to that of the battery void volume. The gases were free to flow in both the battery insulation package, which is nominally 88% void volume and in the GHS, so that this effect is believed to be minimal. Future studies are needed to determine the extent of this effect.

The first gas sample bottle for the control battery (Figs. 1–3) was evacuated and wide open to the previously evacuated and sealed GHS-control battery coupled system when the pyrotechnic was initiated and was then closed nominally 13 s after pyrotechnic initiation to isolate the first gas sample. Times for taking subsequent gas samples can be read directly from the gas composition charts in Figs. 1–6 and from the larger sudden pressure drops shown in Figs. 7 and 8. The smaller sudden pressure drops in Figs. 7 and 8 generally correspond to points where new sample bottles were attached to the GHS and can be associated with negligible amounts of ambient air entering the system. Figures 1–3 show a definite increase in the CH_4 volume fraction for the first 200 s and of the H_2 volume fraction for the first ~50 s in the control battery. During battery operation, the CH_4 volume fraction increases initially, maintains a nominally constant value from 200–600 s, then decreases slowly until about 1200 s, and then remains at a nearly constant value until about 1500 s. Also during control battery operation the CO_2 volume fraction steadily increases for ~200 s starting from 0, decreases fairly rapidly until 600 s, and then decreases more slowly but steadily until about 1500 s.

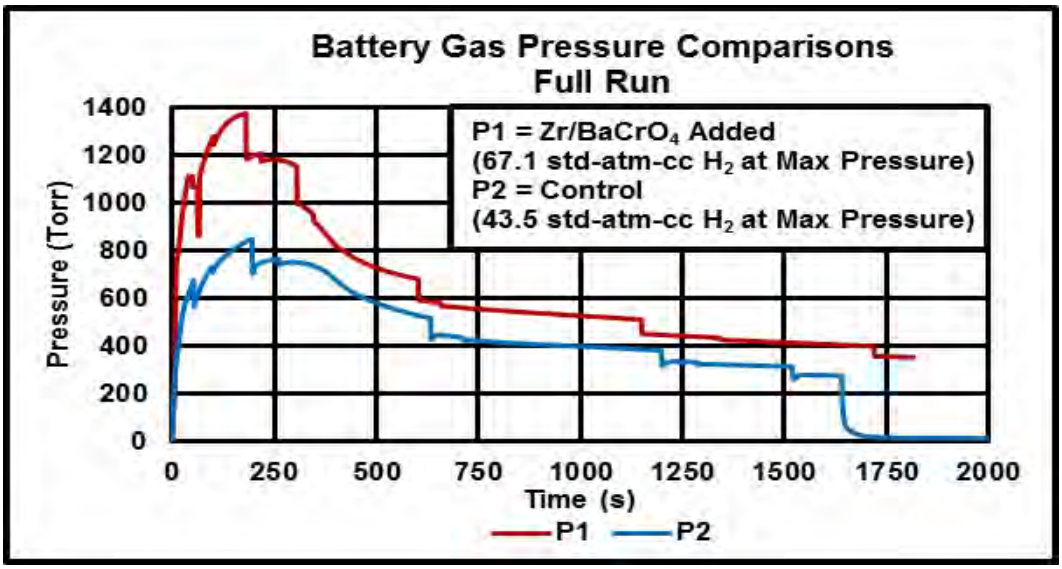

Fig. 7 Pressed pellet thermal battery operating thermal battery gas atmosphere pressure comparisons – Full Run

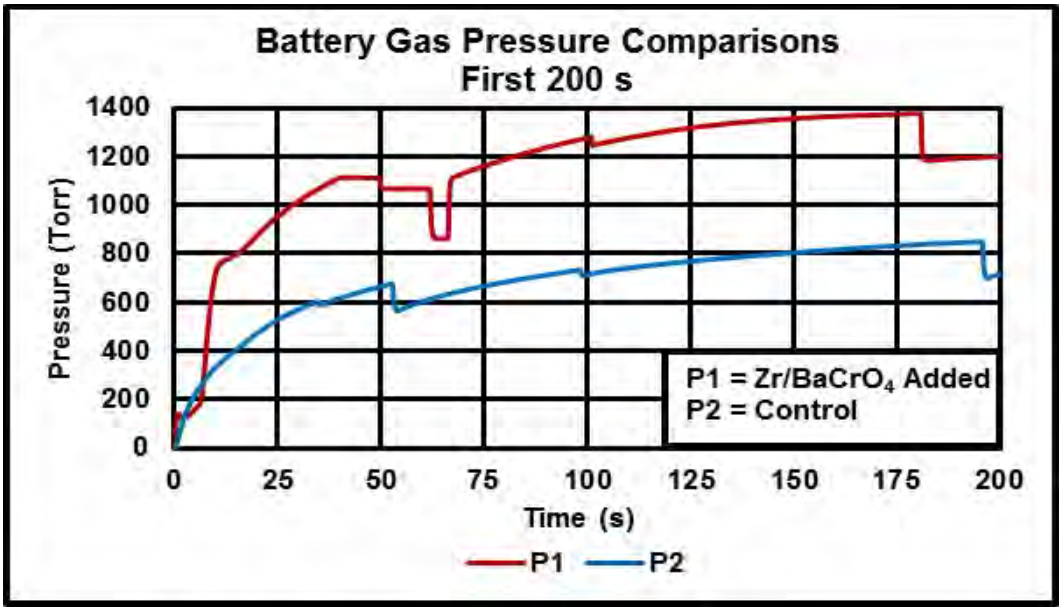

Fig. 8 Pressed pellet thermal battery operating thermal battery gas atmosphere pressure comparisons – First 200 s

The control battery CO volume fraction decreases relatively rapidly from a relatively high initial fractional value of nominally 0.18 at ~13 s until about 200 s following pyrotechnic initiation and then begins to increase slowly. After the control battery electrical operation is complete, the CO_2 gas fraction continues to decline, while the CO gas fraction continues to increase slowly and steadily. Both the O_2 and N_2 gas fractions decline markedly early in battery life and both begin to increase after battery electrical operation is complete.

The first gas sample bottle for the battery containing ~22/78 wt % Zr/$BaCrO_4$ heat paper powder with additional $BaCrO_4$ powder in the thermal insulation package was evacuated and wide open to the previously evacuated and sealed GHS-battery coupled system when the pyrotechnic was initiated and was then closed nominally 15 s after pyrotechnic initiation to isolate the first gas sample (see Figs. 4–6). Note that the H_2 gas volume fraction in Figs. 4 and 6 decreases during the first ~50 s after battery initiation, while it increases during the first ~50 s for the control battery as shown in Figs. 1 and 3. Figures 4–6 show that a lower volume fraction of H_2 and a higher volume fraction of CH_4 was produced for the battery with the heated Zr/$BaCrO_4$ ash than for the control battery shown in Figs. 1–3. For the battery with the heated Zr/$BaCrO_4$ ash, the CO_2 gas fraction was initially present in the first gas sample at a relatively high level instead of starting at 0 as in the control battery, while the CO gas volume fraction was initially lower than for the control battery and remained lower throughout the entire test. For both batteries, the CO volume fraction reaches a minimum at nominally 250 s and then begins to increase slowly but steadily. For the battery with the heated Zr/$BaCrO_4$ ash, the CO_2 volume fraction reaches a minimum at nominally 300 s and then begins to increase steadily, while for the control battery the CO_2 volume fraction declines steadily after a maximum fraction at nominally 200 s. For the battery with the heated Zr/$BaCrO_4$ ash, the O_2 and N_2 gas fractions are much lower than for the control battery throughout the entire test, which suggests that significant amounts of both of those gases have been removed by the heated ash.

During the first ~250 s, the observed interactions of the various gas fractions shown in Figs. 1–6 are consistent with significant burning of organic material for the battery with the Zr/$BaCrO_4$ ash and with the reaction of the Zr/$BaCrO_4$ ash with all of the gases present including the H_2 gas. Large amounts of unmeasured H_2 gas might have been formed and removed in the battery with the heated Zr/$BaCrO_4$ ash since H_2 might have been formed in great excess by the burning organic binder in the thermal insulation. After ~250 s all of the gas volume fractions for both batteries change more slowly, as has been observed previously.

The measured gas pressures and the total H_2 gas volumes evolved at the maximum gas pressures for the 2 batteries are shown in Figs. 7 and 8 (see Fig. 7 text inset). The total quantity of gas produced for the battery with the heated Zr/$BaCrO_4$ ash, originally expected to be much lower than for the control battery, was instead much larger than for the control battery as can be seen directly from Figs. 7 and 8 and confirmed in the detailed gas quantity calculations discussed below.

The battery case temperatures for both batteries are shown in Figs. 9 and 10. Figure 9 (control) shows a typical thermal battery flight case temperature profile sequence with the thin battery case sidewall showing the highest peak temperature,

followed by the case bottom and then by the case header peak temperatures. Figure 10 shows a modified peak temperature profile with the battery case bottom showing the highest peak temperature because the pyrotechnic $Zr/BaCrO_4$ powders were placed next to the metal case bottom. The battery case bottom with the added $Zr/BaCrO_4$ heats much faster and reaches a higher final temperature than does the battery case bottom of the control battery.

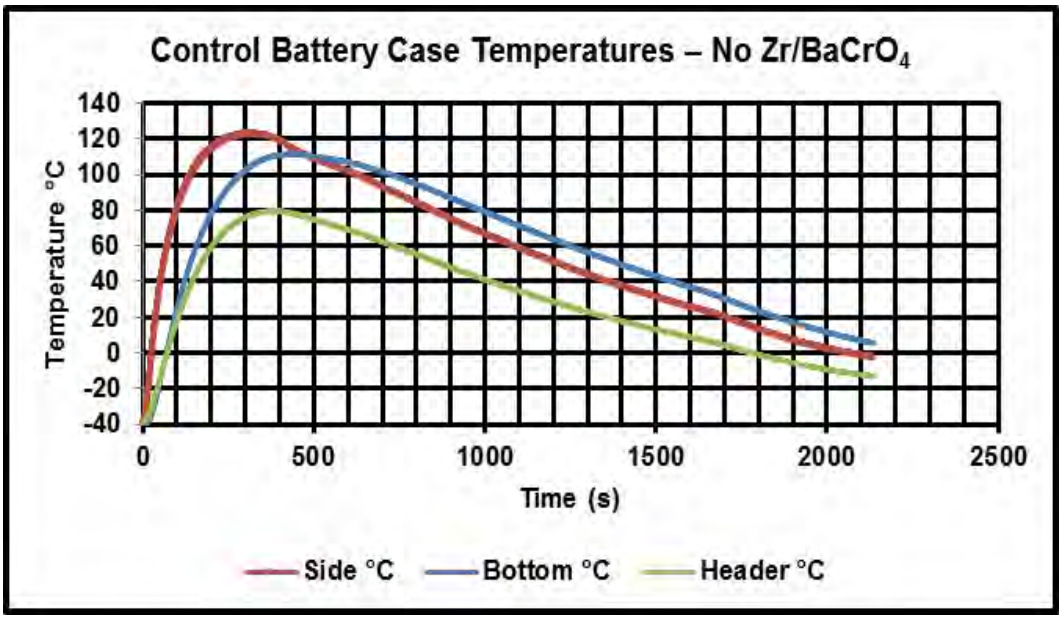

Fig. 9 Control battery case operating temperatures – No $Zr/BaCrO_4$

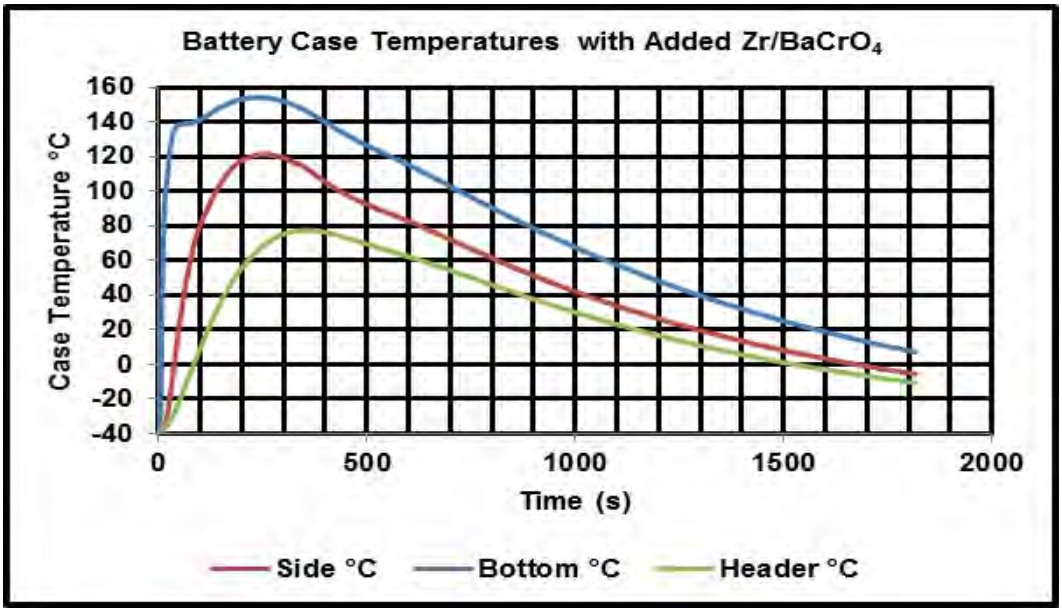

Fig. 10 Battery case operating temperatures with added $Zr/BaCrO_4$ near the case bottom – note the rapid temperature rise and elevated temperature of the case bottom

Because the physical void volumes of the control battery and the battery with the heated Zr/$BaCrO_4$ ash were similar as shown in the detailed calculations below, and because the case temperatures were similar, the gas pressure measurements in Figs. 7 and 8 show immediately that a greater volume of total gas was initially evolved during the heated Zr/$BaCrO_4$ test than during the control test.

The time correlation of gas pressure and the case bottom's sudden temperature rise for the battery with the ~22/78 wt % Zr/$BaCrO_4$ with additional $BaCrO_4$ placed near the case bottom (Figs. 8 and 10) is shown in Fig. 11. Data for Figs. 7–11 were taken at intervals of ~0.1 s and individual data points can be seen in those figures on the time scales shown in this report only when pressures or temperatures change rapidly with time. The initial evacuated pressure was the nominal 50 microns of mercury (~6.7 Pa) pressure of the sealed GHS and the initial temperature was the –40 °C of the battery case and temperature chamber.

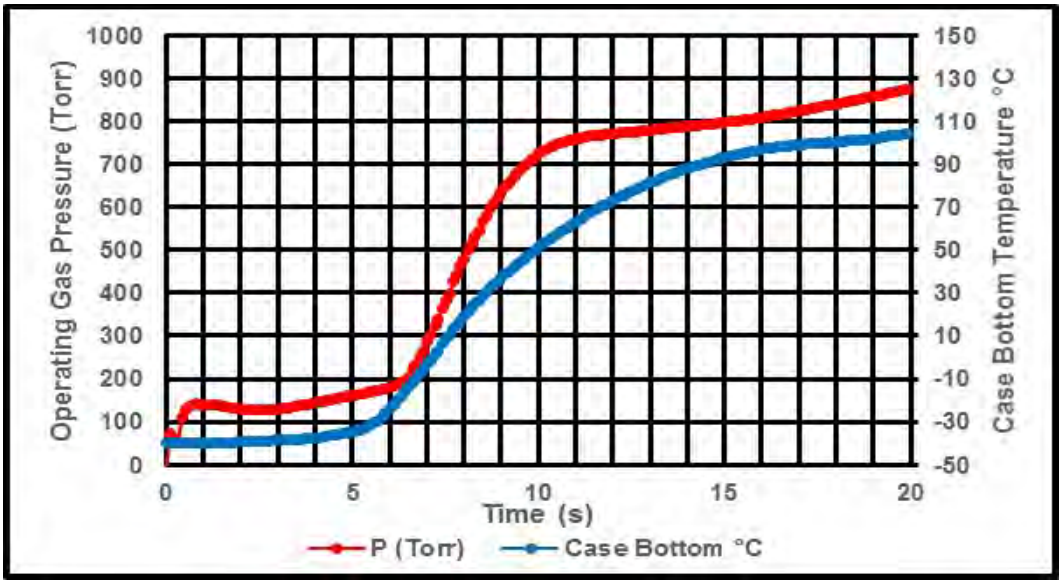

Fig. 11 Time correspondence of battery case bottom temperatures and gas pressures for the battery with Zr/$BaCrO_4$ in the case bottom

The ~5 s delay time between the initial pressure rise and the subsequent rapid rise of both case temperature and case pressure shown in Fig. 11 most likely indicates a delayed ignition of the Zr/$BaCrO_4$ mixture in the battery case bottom. Such a late firing might have been partially or wholly caused by a pyrotechnic dilution effect from the excess $BaCrO_4$ that was added to the 22/78 Zr/$BaCrO_4$ heat powder mixture. As noted above, dilution of the Zr/$BaCrO_4$ heat powder with additional $BaCrO_4$ might also be related to the apparent inability of the resulting Zr/$BaCrO_4$ ash to remove significant amounts of H_2 gas from the battery operating atmosphere because a sufficiently high ash temperature was not reached when the Zr/$BaCrO_4$

powder mixture was ignited. The slower but still rapid gas pressure rise from ~10 to ~40 s might be caused by initial high temperature burning of the organic binder materials in the thermal insulation after initiation of the pyrotechnic powder.

5. Standard Temperature and Pressure (STP) Gas Volume Calculations

Evolved gas volumes were determined using the ideal gas law with the pre-measured internal volumes of the GHS and the test battery void volumes along with the gas pressures, battery case temperatures, and GHS temperatures measured during battery operation. The battery operating thermal cell stack temperatures were not measured directly, but were assumed to be near 500 °C on the bases of previous experience and thermal modeling. Calculated volumes of H_2 gas actually evolved for the 2 batteries during battery operation and the formulas used for the calculations are shown in Figs. 12–15.

The total amount of H_2 gas evolved at maximum gas pressure was ~43 std-atm-cc for the control battery and ~67 std-atm-cc for the battery with the heated Zr/$BaCrO_4$ powders with a nominal ±10% accuracy for both tests (Figs. 12–15). Some of the calculations shown in Figs.12–15 are confirmation calculations using alternate calculation methods. As mentioned above, it is possible that more H_2 was generated from the test with the heated Zr/$BaCrO_4$ powders than was measured and that this unmeasured H_2 was removed by the Zr/$BaCrO_4$ powder ash. If all of the CH_4 in the battery with the heated Zr/$BaCrO_4$ were formed from evolved H_2 and if no additional H_2 were formed except for the H_2 present as H_2 and as CH_4, then the total maximum amount of H_2 evolved in the Zr/$BaCrO_4$ powder ash battery would have been 131.6 std-atm-cc. For the control battery, the corresponding maximum amount of H_2 evolved would have been 71.5 std-atm-cc.

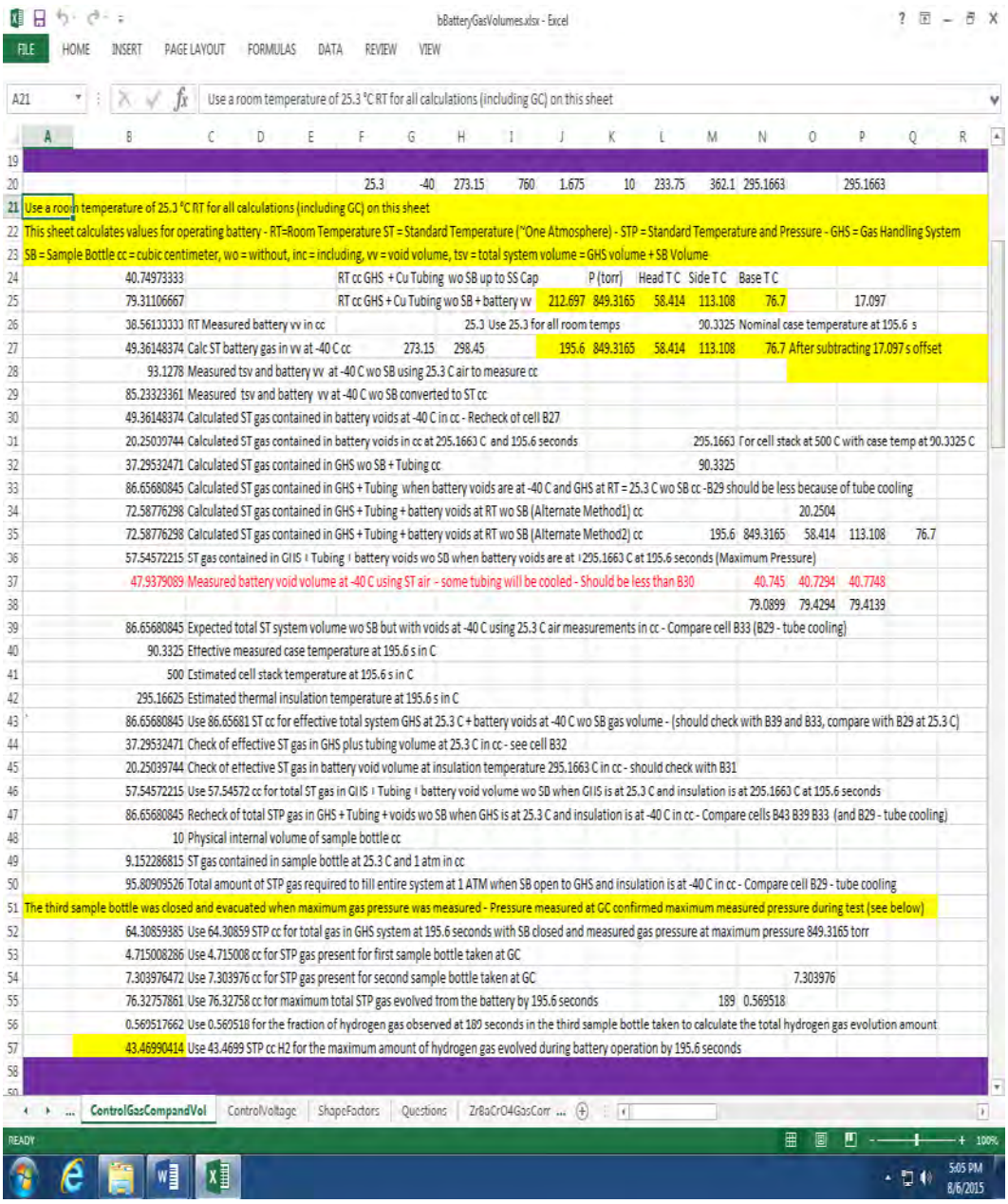

Fig. 12 STP calculated gas evolution volumes – Control battery

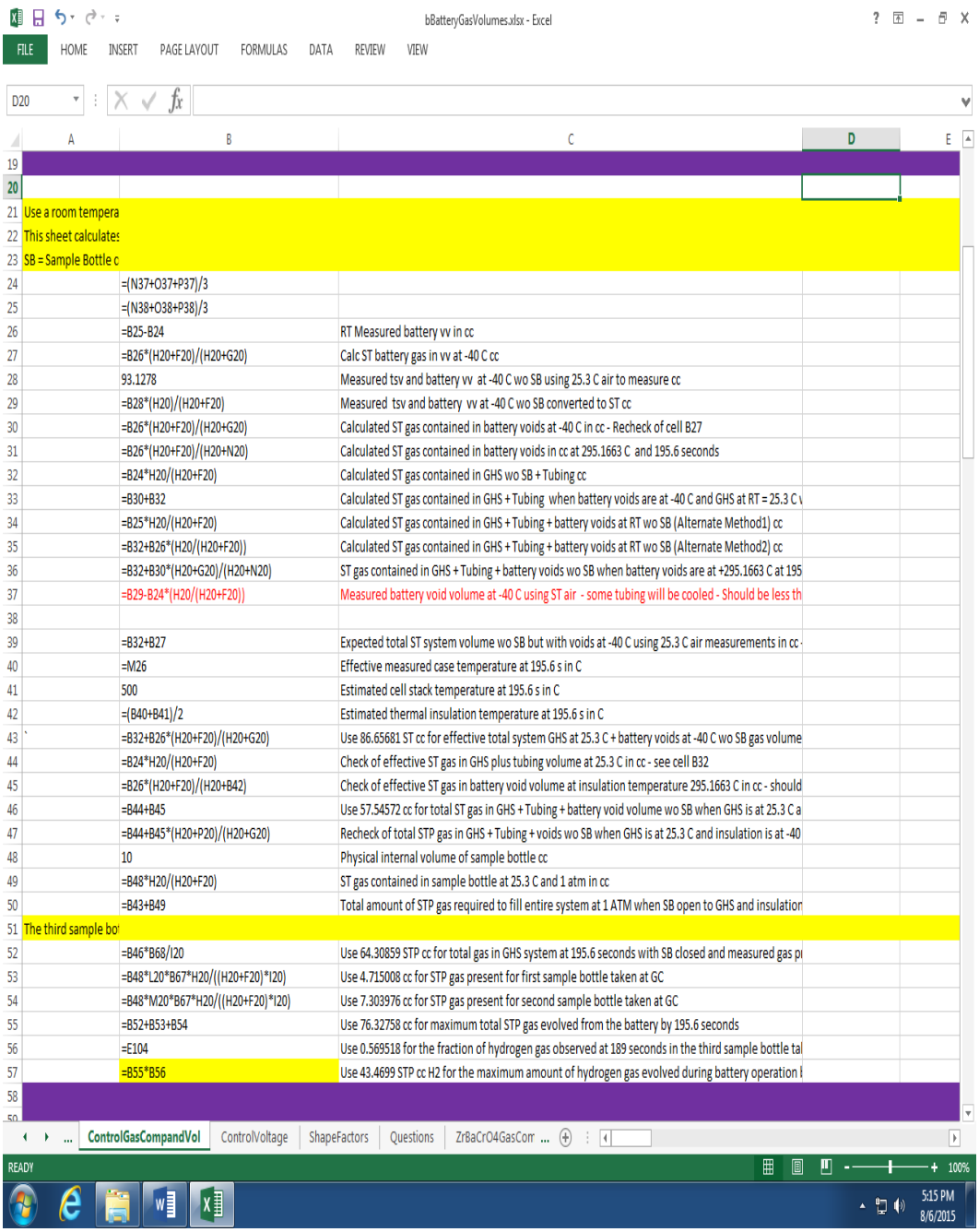

Fig. 13 Formulas for STP calculated gas evolution volumes – Control battery

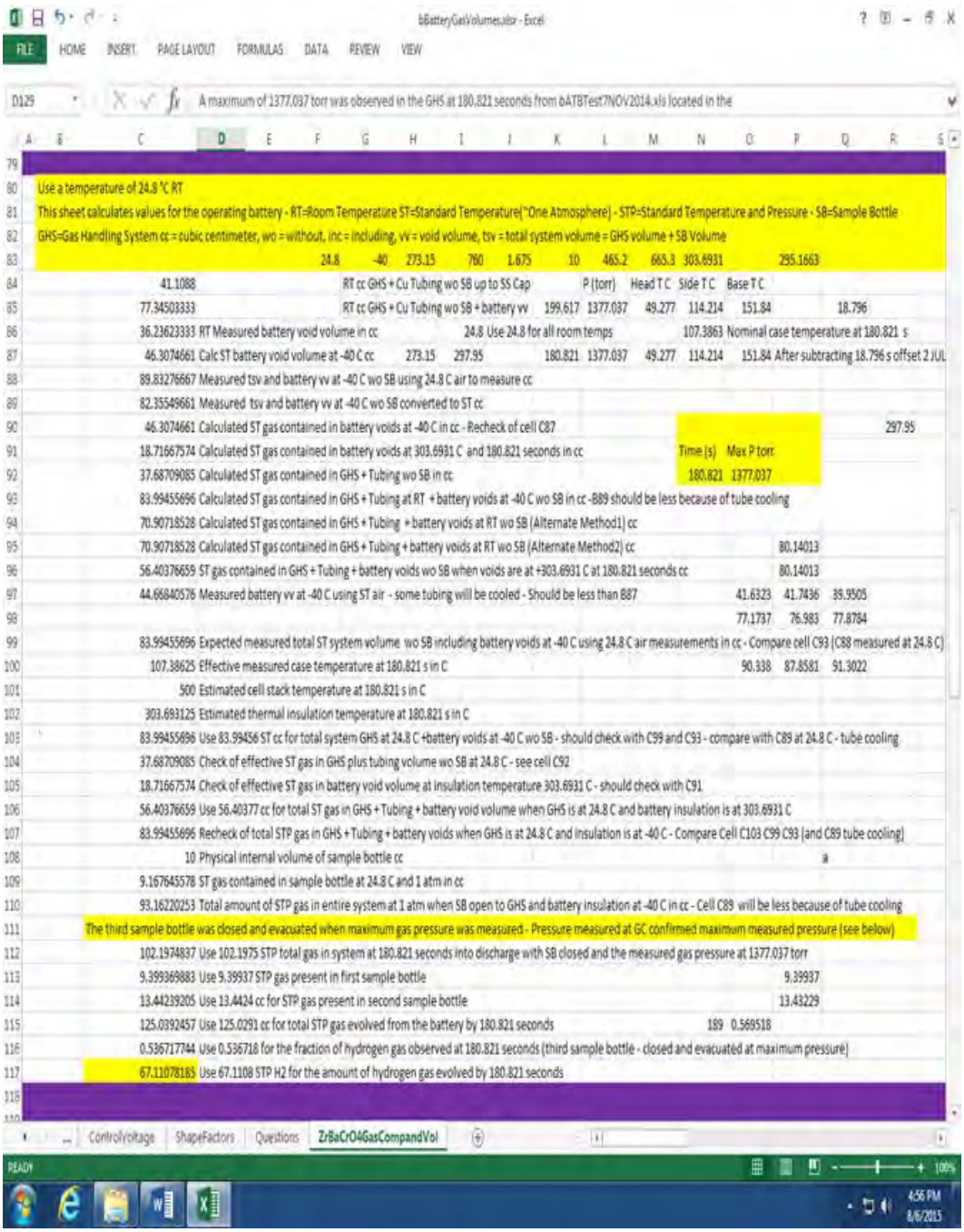

Fig. 14 STP calculated gas evolution volumes – Battery with heated Zr/$BaCrO_4$ powder ash

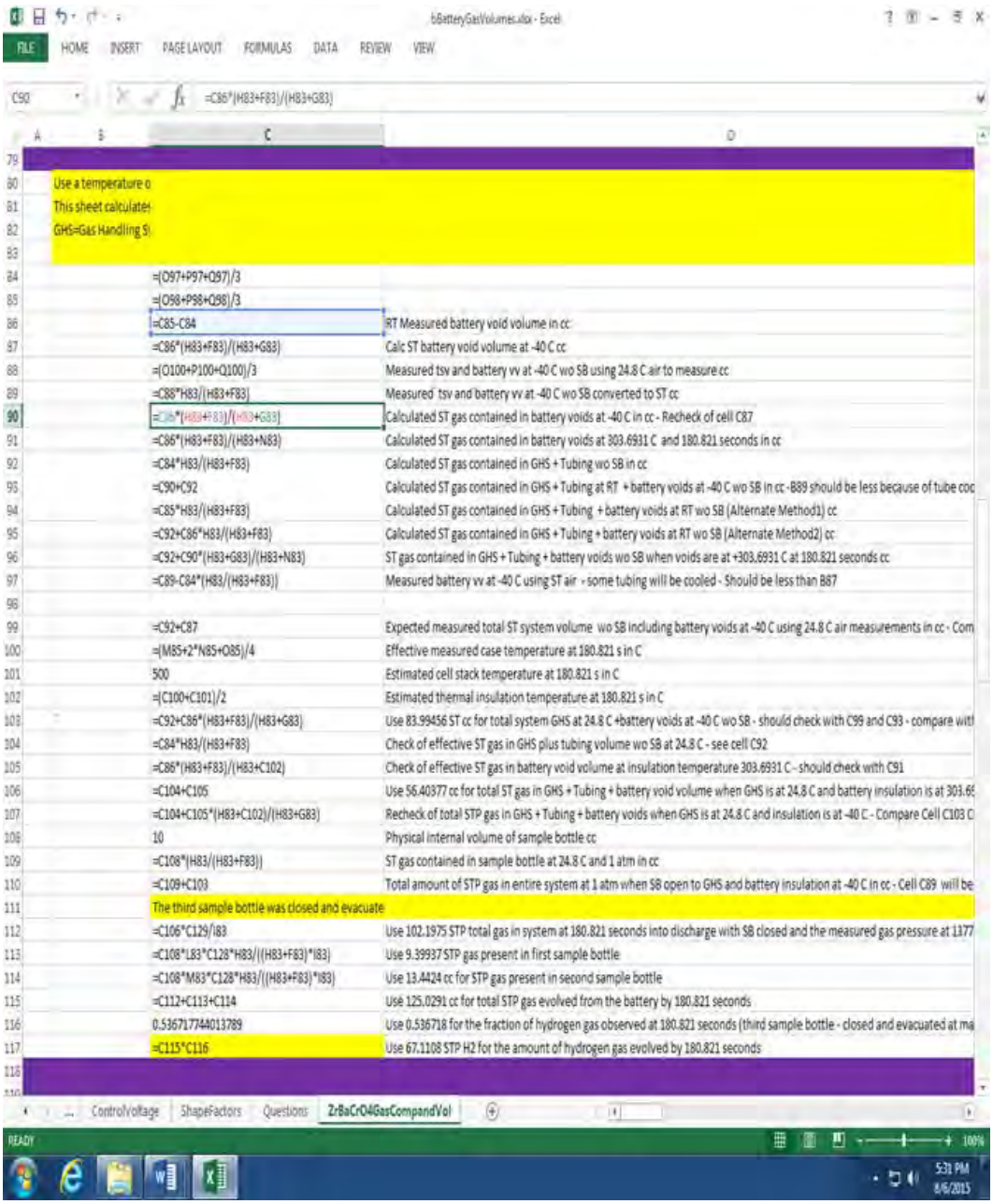

Fig. 15 Formulas for STP calculated gas evolution volumes – Battery with heated Zr/$BaCrO_4$ powder ash

6. Thermal Modeling Calculations – ARL Fortran Programs – Sierra Finite Element Models – Paraview Visualization

The preferred geometric configuration for pressed pellet thermal batteries is the right circular cylinder. The axisymmetric Sierra TABS finite model elements (displayed as planar elements in the thermal model) reduce calculation time, and Sierra TABS heat losses are calculated as if the cylinder sides were mathematically

radial. Heat losses through the thermal insulation packages are calculated by the use of geometric shape factors in the ARL/Adelphi Fortran programs. The Sandia Sierra TABS finite element models and the ARL/Adelphi Fortran programs were found to be numerically equivalent when calculating thermal battery lifetimes and heat loss rates through the thermal insulation packages, while mathematically rigorous calculations of planar transient thermal insulation heat transfer agreed numerically with ARL developed finite element models.[1] Steady-state heat transfer calculations for planar and cylindrical coordinates can be compared easily, but the comparison of transient state calculations in 3 dimensions is less intuitively obvious and can be communicated more explicitly using the Paraview finite element visualization programs. Sandia originally developed their programs using the internal plotter software as a visualization tool (Figs. 16–18) and later added the more comprehensive Paraview software visualization (Figs. 19 and 20). Figures 21–24 are Excel charts using digital data taken from Sierra TABS finite element models. All calculations in Figs. 16–21 used 0.1-s burn times.

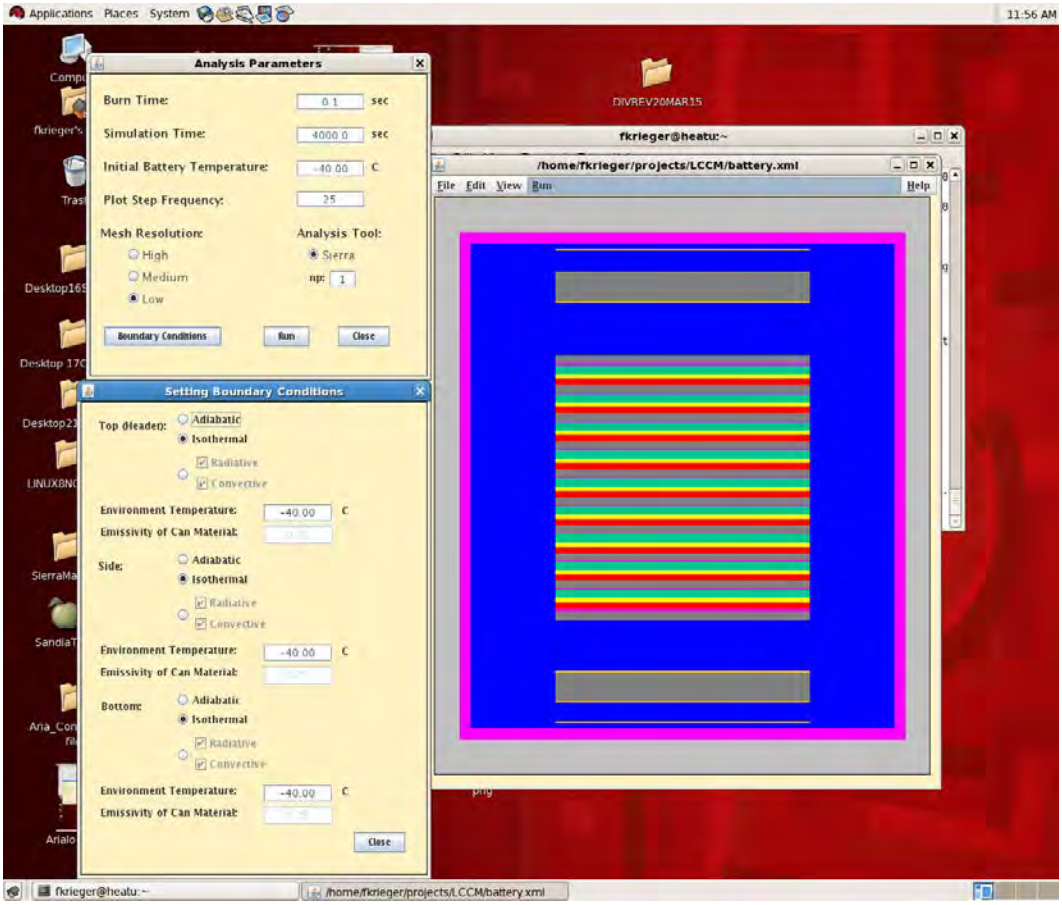

Fig. 16 Sierra TABS Internal Plotter – Final pre-processing step for Low Cost Competent Munition (LCCM) thermal battery (battery shown drawn to scale)

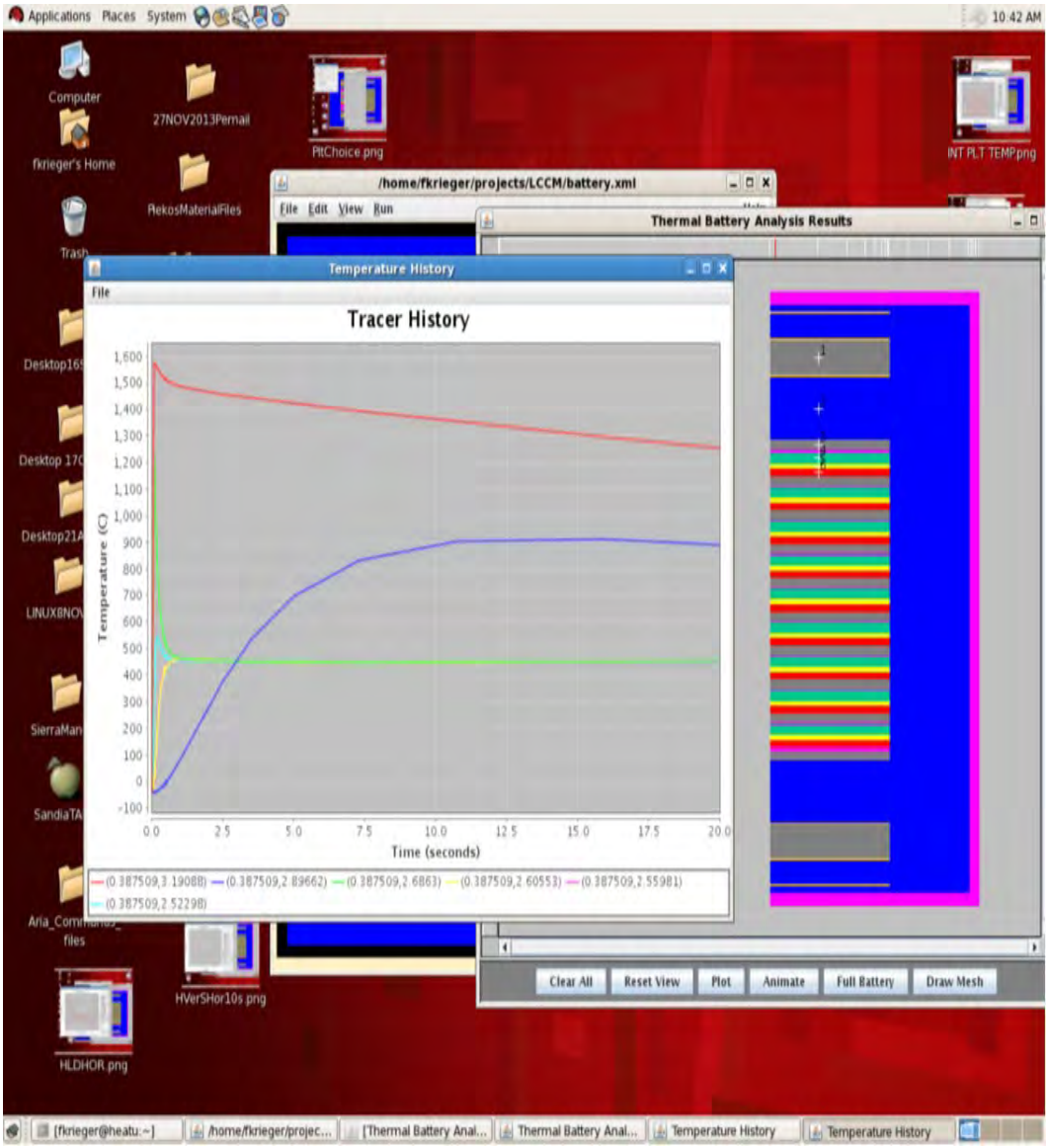

Fig. 17 Sierra TABS Internal Plotter – Individual points selected – Temperature-time LCCM curves after pyrotechnic initiation

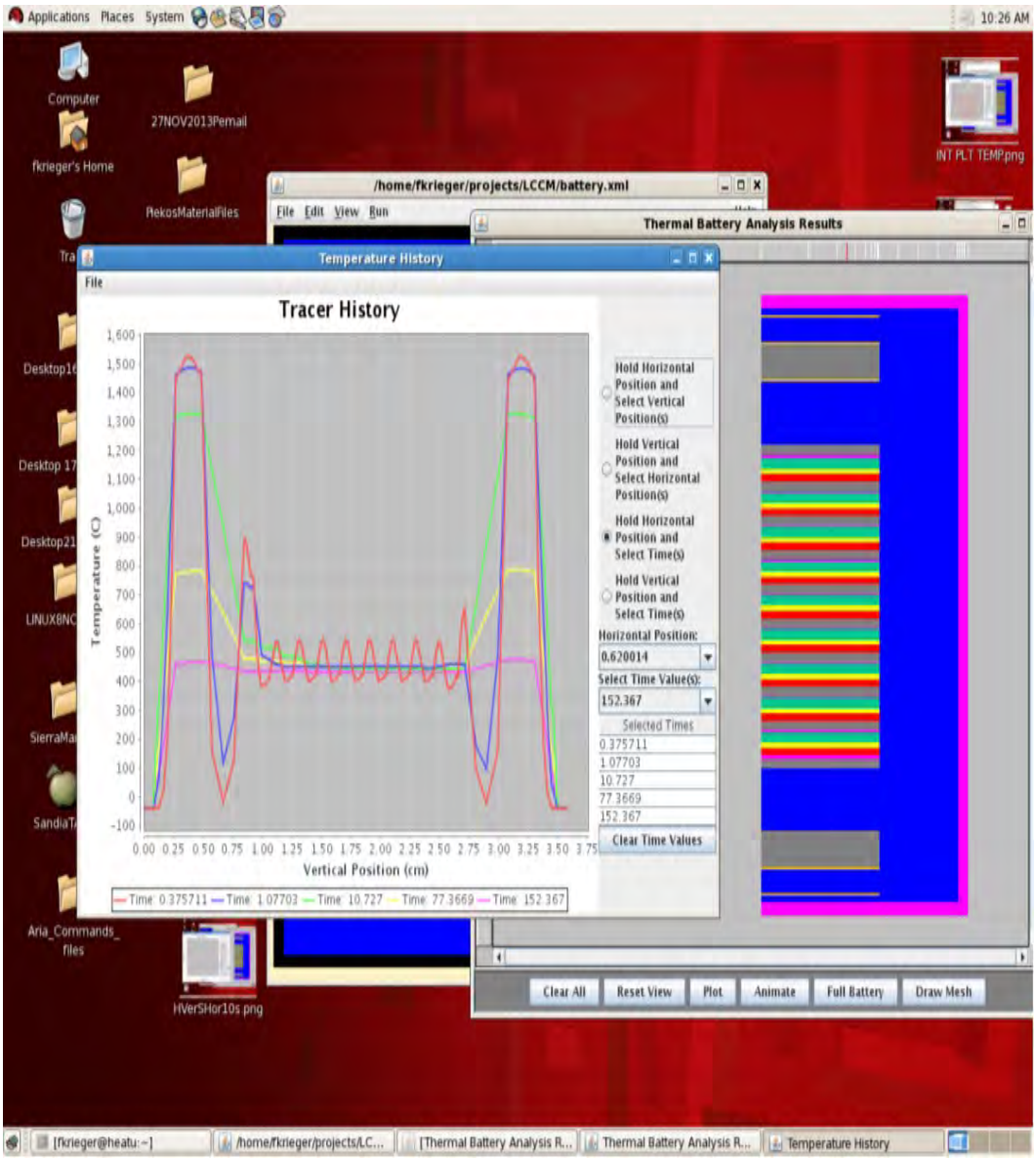

Fig. 18 Sierra TABS Internal Plotter – Series of LCCM points selected and plotted for selected times after pyrotechnic initiation

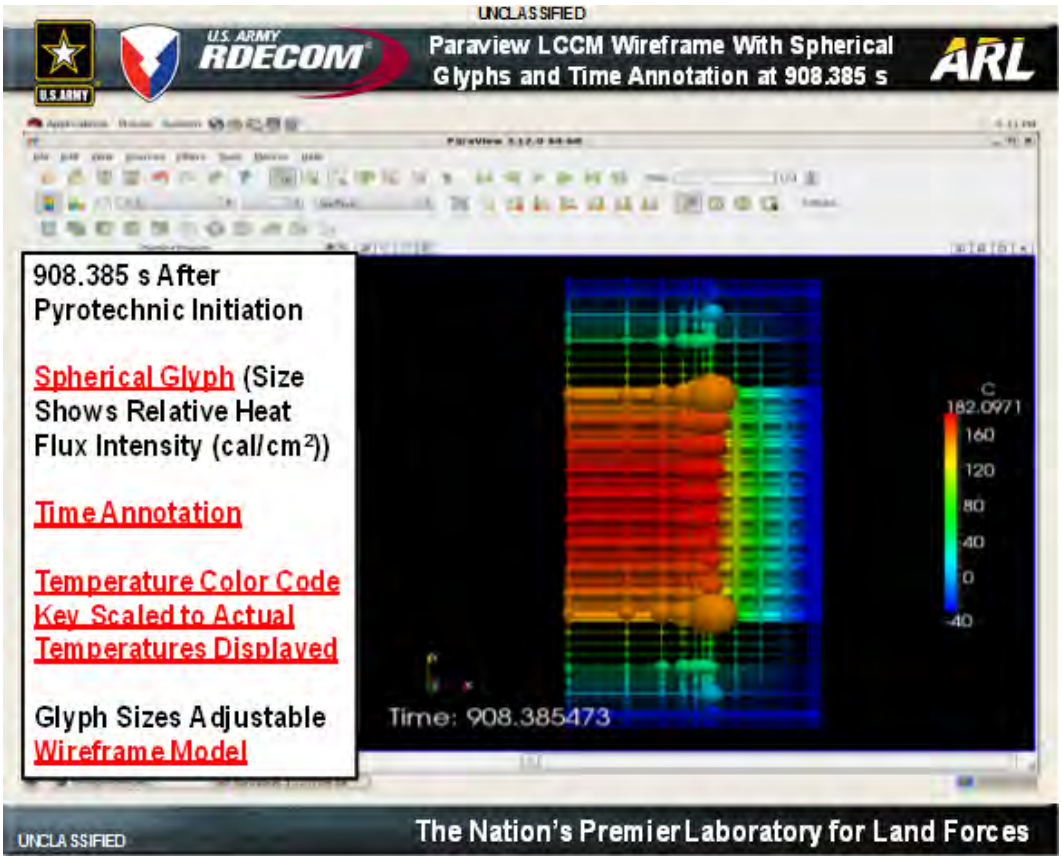

Fig. 19 Sierra TABS LCCM calculation results – Paraview with spherical glyphs – Spherical sizes are proportional to heat flux – Overall spherical size scales are adjustable

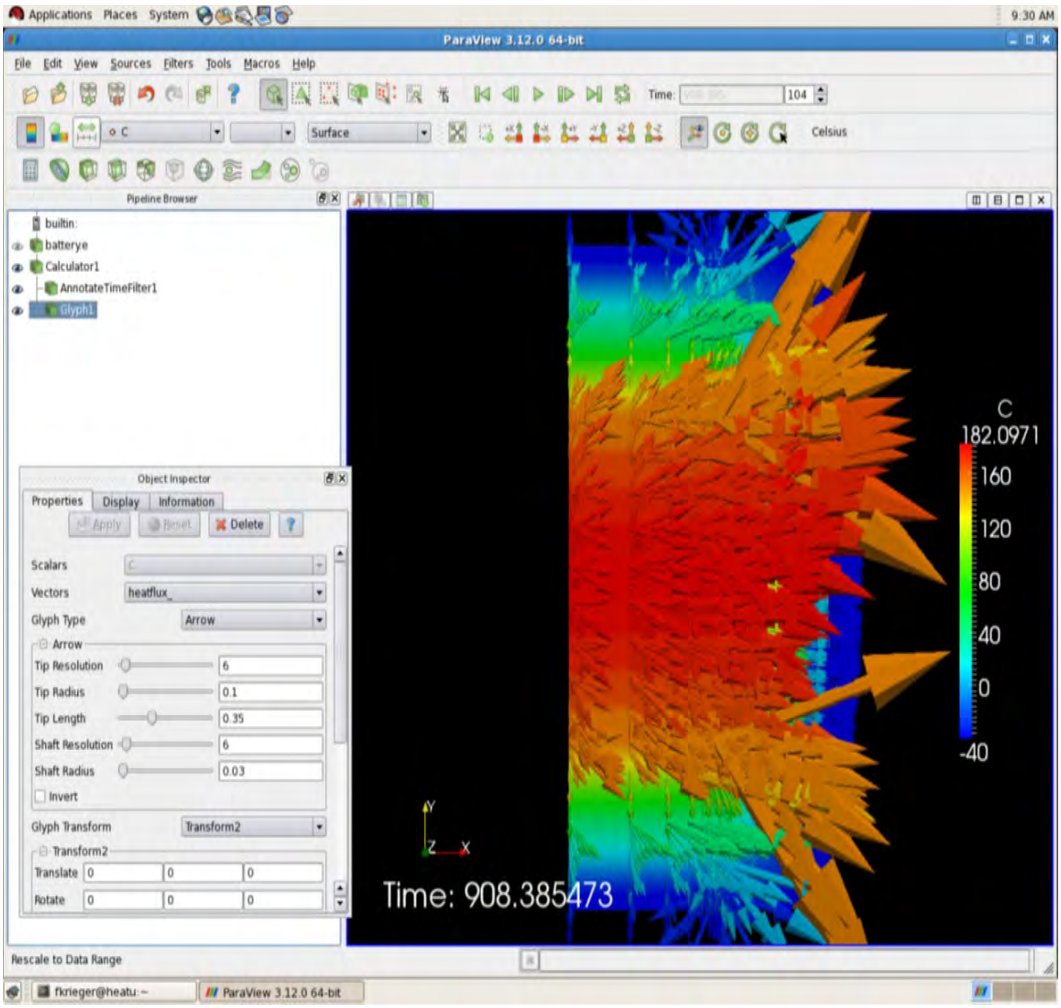

Fig. 20 Sierra TABS LCCM calculation results – Paraview with arrow glyphs – Arrow sizes are proportional to heat flux – Overall arrow size scales are adjustable

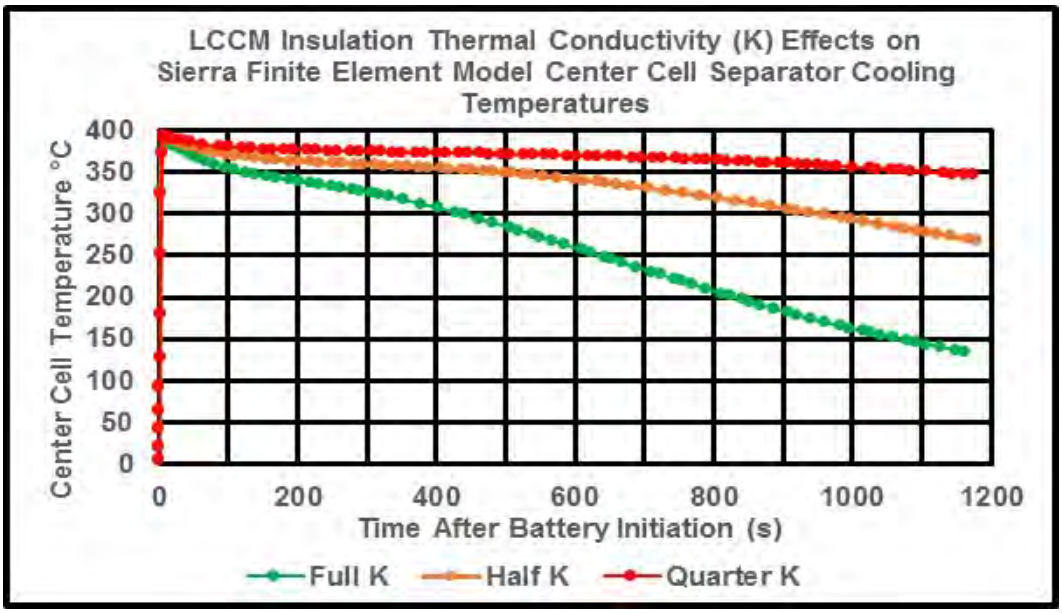

Fig. 21 Sierra TABS – Calculated LCCM center cell separator cooling times

The Full K LCCM thermal battery cooling curve in Fig. 21 used a brochure thermal conductivity value for a commercial thermal insulator with a 60/40 vol % H_2/air atmosphere filling the porous insulation structure. This K value was then divided by 2 and then by 4 to get the Half K and Quarter K curves to demonstrate the potential effects of H_2 removal and of reducing the thermal conductivity of the insulation package. All of these curves used a pyrotechnic burn time of 0.1 s.

The same (single) point was used for the all 3 of the curves shown in Fig. 21 (near the axial center and radially nearly midway between the thermal cell center and outer diameter of the separator layer in the center cell of the LCCM thermal cell stack [see Fig. 16]). As mentioned above, small temperature variation measurements within the thermal cell stack might be combined with DOE statistical techniques to investigate electrochemical and thermodynamic reactions occurring within the cell stack that are of significant importance to improved thermal battery operation. Control of heat generation within the thermal cells themselves, for example, would greatly improve present thermal battery lifetimes and energy densities.

7. Sierra TABS Analyses of Fast Rise Thin-Film Thermal Batteries

Fast rise thin-film thermal batteries have been proposed for small close-quarter munitions and for armor and bunker penetrating munitions of the future. The Sierra TABS finite element model permits small burn times to be written into the model.

Very small thermal battery burn times are available when using fast-burning pyrotechnic materials such as Nanofoil™ that have recently become available[6–8] and the use of such materials can be effectively modeled in Sierra TABS.

The nominal burn rate of heat pellet pyrotechnic in a pressed pellet thermal battery is 5 in./s (0.2 s/in.) while the nominal burn rate of the nickel aluminum (NiAl) Nanofoil pyrotechnic proposed for use in the fast rise thin-film thermal battery is 30 ft/s (0.00277778 s/inch). Using a pressed pellet thermal battery with the diameter of the LCCM pressed pellet thermal battery (0.75 inch) the nominal burn time of the pyrotechnic heat pellet for a fuse strip located at 1 point on the cell diameter would be 0.2 s/inch x 0.75 inch = 0.15 s. The corresponding nominal burn time for the Nanofoil heat source would be 0.00277778 s/inch x 0.75 inch = 0.002083 s. If the fuse strip covered the entire cell stack circumference or if the thermal battery used center hole ignition the burn times directly above would both be divided by a nominal factor of 2. The large number of calculated mathematical points shown below in curves (Figs. 22–24), combined with the short burn time of 0.002083 s, show the comprehensive mathematical potential and robust nature of the thermal model. The same single point was used in Figs. 22–24, as indicated in the figure captions.

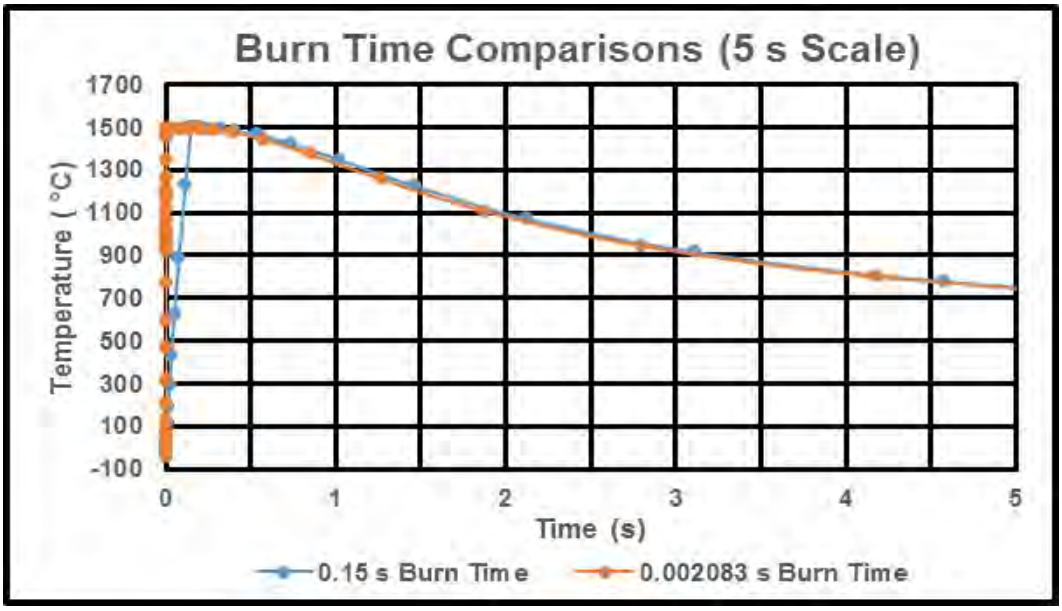

Fig. 22 Comparison of calculated temperature rise time curves with 0.15- and 0.002083-s burn times – Sierra TABS (point near axial center and nearly midway between radial center and outer diameter of top heat pellet in thermal cell stack) – First 5 s

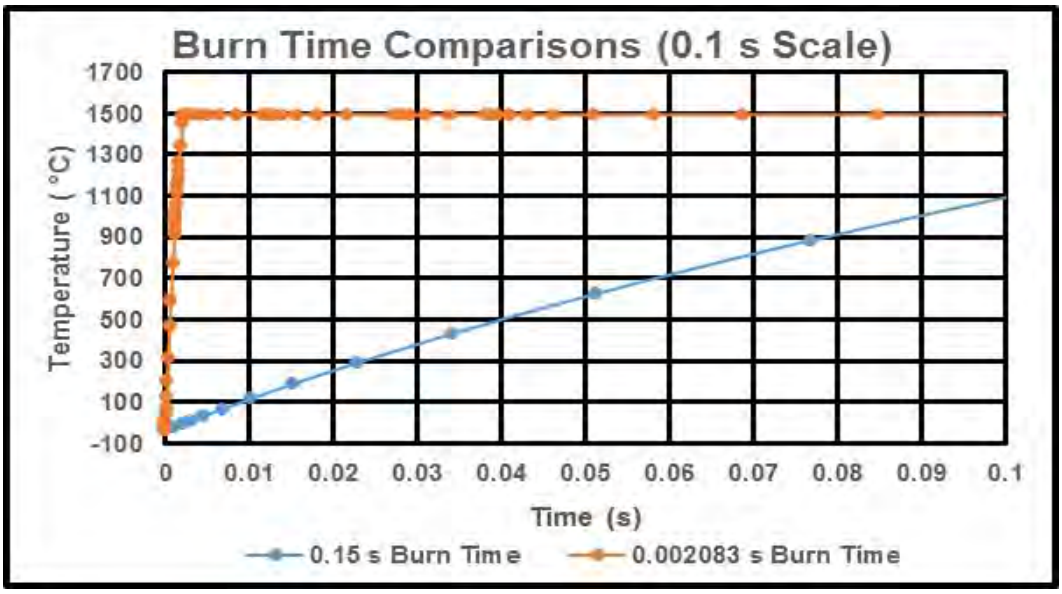

Fig. 23 Comparison of calculated temperature rise time curves with 0.15- and 0.002083-s burn times – Sierra TABS (point near axial center and nearly midway between radial center and outer diameter of top heat pellet in thermal cell stack) – First 0.1 s

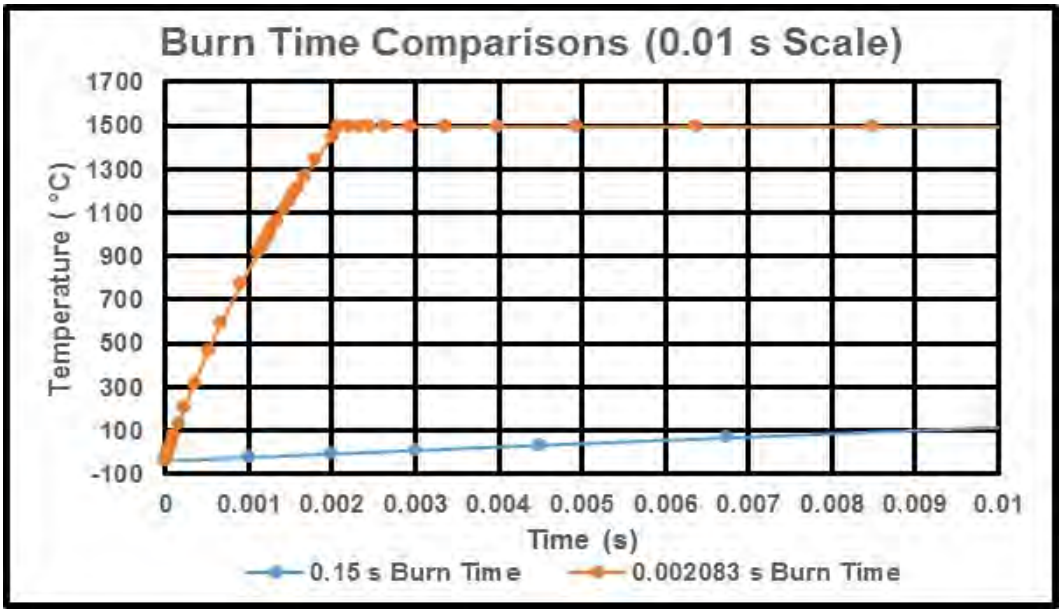

Fig. 24 Comparison of calculated temperature rise time curves with 0.15- and 0.002083-s burn times – Sierra TABS (point near axial center and nearly midway between radial center and outer diameter of top heat pellet in thermal cell stack) – First 0.01 s

Paraview software permits a wide range of zoom and individual point and element selection capabilities. Figure 25 shows a Paraview visualization of an LCCM thermal battery using a burn time of 0.002083 s where only the heat source elements (block 3) are displayed with arrow glyphs for heat flux visualization. In general, any single point or element or combination of points or elements may be chosen in

Paraview and the value of any parameter included in the model can be displayed for any selected points or elements at any time throughout the calculation interval.

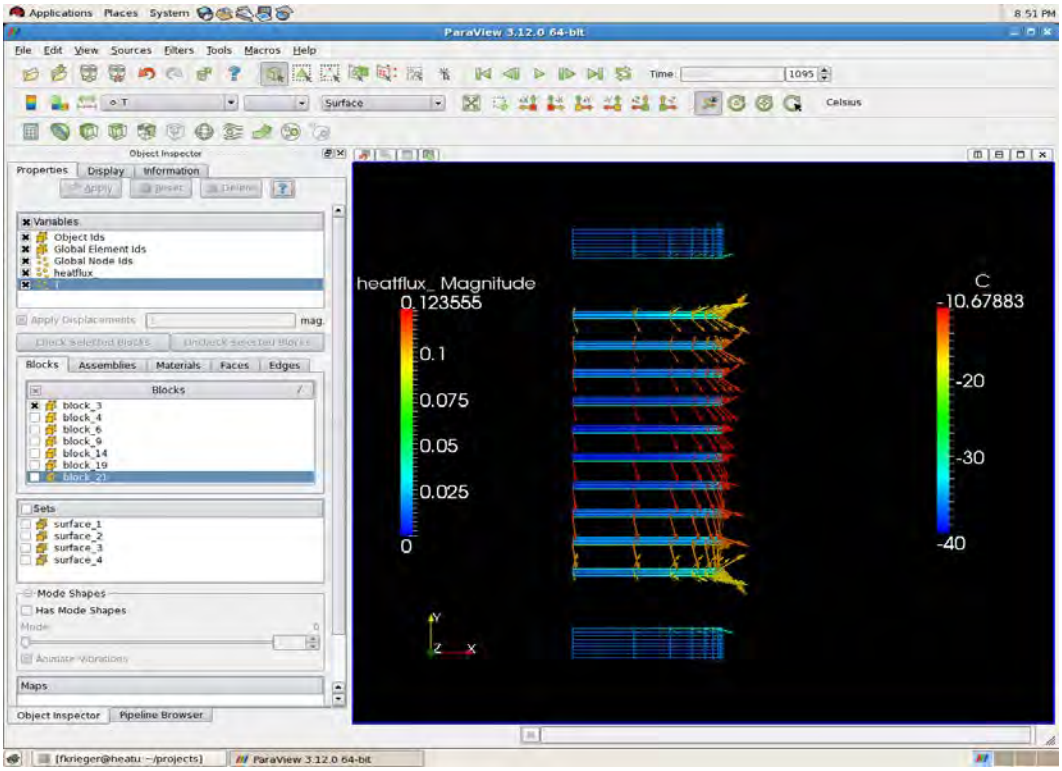

Fig. 25 Paraview heat flux visualization (arrows) with nominal Nanofoil burn rates (30 ft/s)

8. Gas Collection Methods – Gas Collection from Laboratory Test and Flight Test Thermal Battery Cases

A previously reported hermetically sealed reusable SS test fixture for LCCM laboratory thermal battery experimentation (Fig. 26, left) has been used for electrical output and gas evolution testing of laboratory type thermal batteries, but the method is labor intensive and time consuming.[5] The reusable test fixture shown in Fig. 26 is thick walled and massive by design so that the temperature rises minimally during battery discharge, which permits battery operation to be measured under "worst case" heat sink conditions. The thick-walled battery case also permits standard hermetic sealing methods to be applied for the collection of evolved gases. The corresponding LCCM flight test thermal battery is packaged into a thin-walled flight case (Fig. 26, right), which is also made using SS.

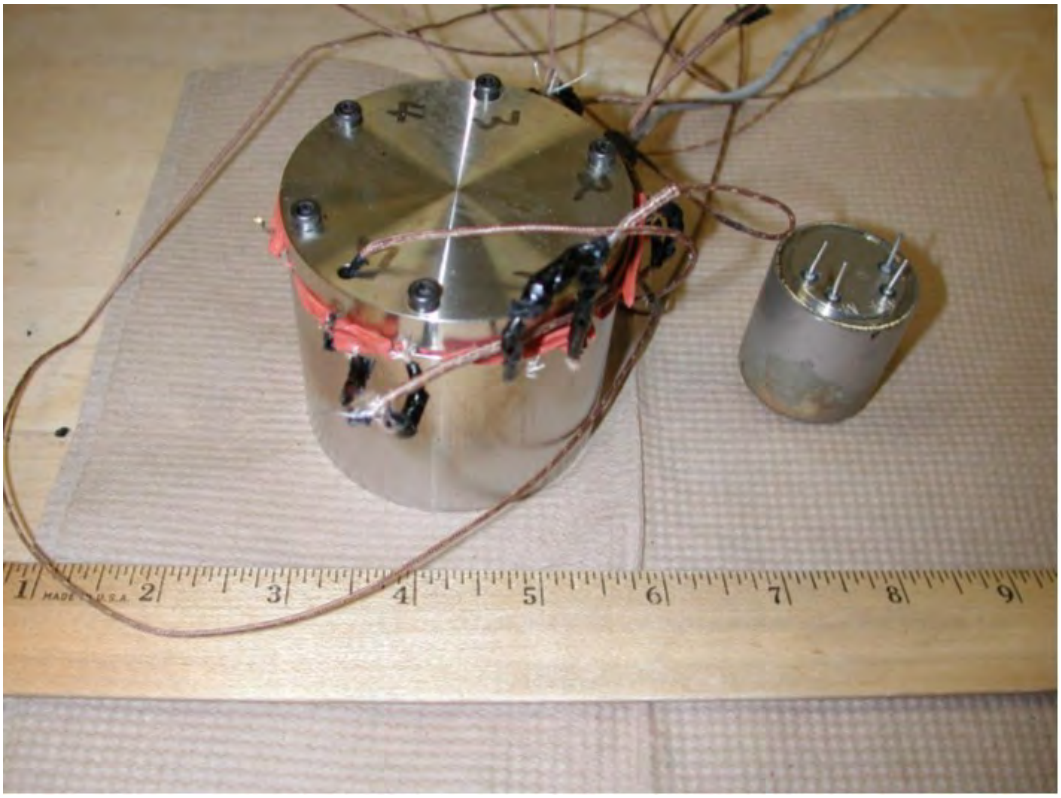

Fig. 26 LCCM thermal battery cases: thick-walled SS laboratory test fixture (left) and thin-walled SS flight case (right)

9. Gas Collection Methods – Gas Collection from Production Type Thermal Batteries with Attachable Standard Gas Fittings

Thin-walled SS cases are typically used in munitions thermal batteries to reduce total thermal battery mass, and titanium cases are sometimes used to further reduce total thermal battery mass. Because of their low mass and thermal capacity, thin-wall thermal battery cases may reach high case temperatures (200–400 °C) during battery operation if the batteries are thermally isolated from their surroundings. Such battery case temperatures may approach or exceed the melting point of the molten salt electrolyte in the thermal cell stack and can damage temperature-sensitive internal thermal battery components. Because of the high case temperatures often measured during battery discharge, significantly elevated temperatures are ordinarily required to form hermetic seals that will remain effective at those required high operating battery case temperatures. Acceptable hermetic seals for thermal batteries ordinarily use laser welding, tungsten inert gas (TIG) welding, or high temperature (~1000 °C) melting point silver solder methods.

Thin-walled thermal battery cases can be hermetically sealed for gas collection experiments without damaging temperature sensitive internal thermal battery components if special gas fittings are properly attached to the case prior to battery assembly. After battery assembly, cases with these special fittings can then be easily connected directly to a GHS to test gas evolution during battery operation.

It should be noted that thin-walled thermal battery cases are often in direct contact with much larger metal SS or aluminum external heat sinks when assembled into munitions. When such batteries are assembled into such a munition, the operating battery ordinarily produces lower case temperatures similar to those that will be reached with the above described "worst case" reusable test fixture heat sink. Munitions thermal battery operation is ordinarily evaluated both with the battery case thermally isolated from the surrounding environment and with the battery case assembled within the ordnance round or an equivalent mass steel or aluminum test fixture (with and without an external heat sink).

10. Gas Collection Methods – Gas Collection from Production Type Thermal Batteries When Standard Gas Fittings Are Not Easily Attached

Effective high temperature attachment of standard gas collection fittings using high temperature attachment methods such as laser welding with external battery case heat sink fixtures and a knowledge of the placement of the internal components in the battery should first be considered. If these methods are not appropriate, initial levels of gas compositions and amounts immediately after thermal battery initiation can nevertheless be estimated for such thermal batteries simply by drilling a hole in the battery case bottom while the battery is in a dry room or glove box atmosphere and providing a gas tight seal using materials such as high temperature silicone rubber gaskets mechanically clamped to the case bottom. The initial gas sample or samples collected before significant heating of the gasket will show the initial gas atmosphere of the operating thermal battery. Later during battery operation as the case temperature increases, O_2 and N_2 gas may enter the operating battery gas atmosphere (either from a loss of the hermetic seal or from out-gassing of the gaskets) but a significant amount of useful information on battery gas evolution characteristics will already have been obtained.

The gas composition throughout battery discharge during normal operation can then be estimated from a knowledge of the initial gas composition, a knowledge of the materials within the battery, the measured battery case temperatures, internal measured gas pressures and compositions, and previous testing experience with similar batteries. It should be noted that at sufficiently high temperatures the gaskets

might degrade further and contaminate the gas atmosphere with volatile degradation products and with the ambient atmosphere.

An actual gas evolution test of a pressed pellet production thermal battery tested in this manner with silicone rubber gaskets is shown in Fig. 27. The temporary hermetic seal with the silicone rubber gasket was confirmed experimentally before battery initiation. After battery initiation into a previously evacuated, coupled, and hermetically sealed battery void-GHS system as explained above, the evolved gas N_2 and O_2 values in Fig. 27 both start near 0% volume fraction as expected. This strongly indicates that the silicone rubber gasket seal remained hermetic for several seconds after battery initiation and that the evolved gas composition and quantity measured for the first gas sample taken at ~12 s after battery initiation is correct. As noted above, most pressed pellet thermal batteries show nominal H_2 fractions of 60–80 vol %, so that this test shows immediately that no effective H_2 gas control has been used for this battery.

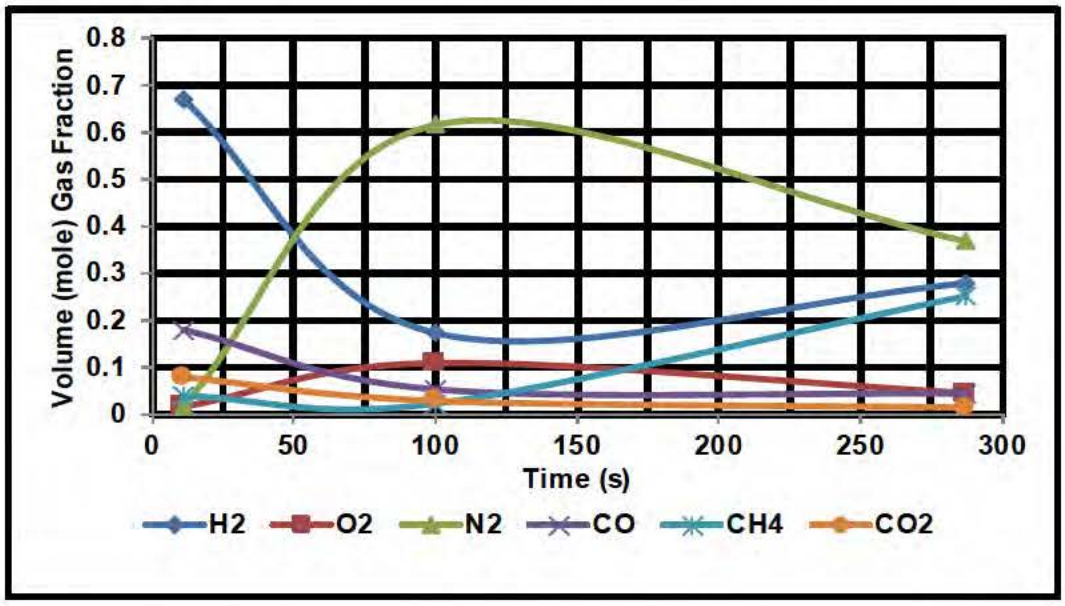

Fig. 27 Thin-wall case thermal battery gas evolution test using silicone rubber gaskets with mechanical clamps to form an initially hermetic thermal battery case gas seal

11. Proposed Test Fixture for Rapid Tests of Laboratory Thermal Batteries

The simplified laboratory thermal battery test fixture shown below (Figs. 28–30) is easily hermetically sealed and will have adjustable radial and axial SS inserts for testing various internal case dimensions. This easily exercised control of the internal case dimensions greatly facilitates rapid construction and simplifies heat balancing of the thermal insulation package. Case dimensions can be rapidly

adjusted to available insulation thicknesses and required insulation taping can be minimal or nonexistent. The simplified test fixture can also be modified to routinely measure the axial mechanical force on the thermal cell stack during discharge, which affects battery discharge capabilities and has not been appropriately measured in most previous tests. The actual hermetic sealing and collection of gas samples with the modified test fixture would be done using similar methods to those previously reported.[1–5] The internal construction of the lid and the geometry of the load cell would insure accurate measurements of thermal cell stack axial pressures during thermal battery discharge.

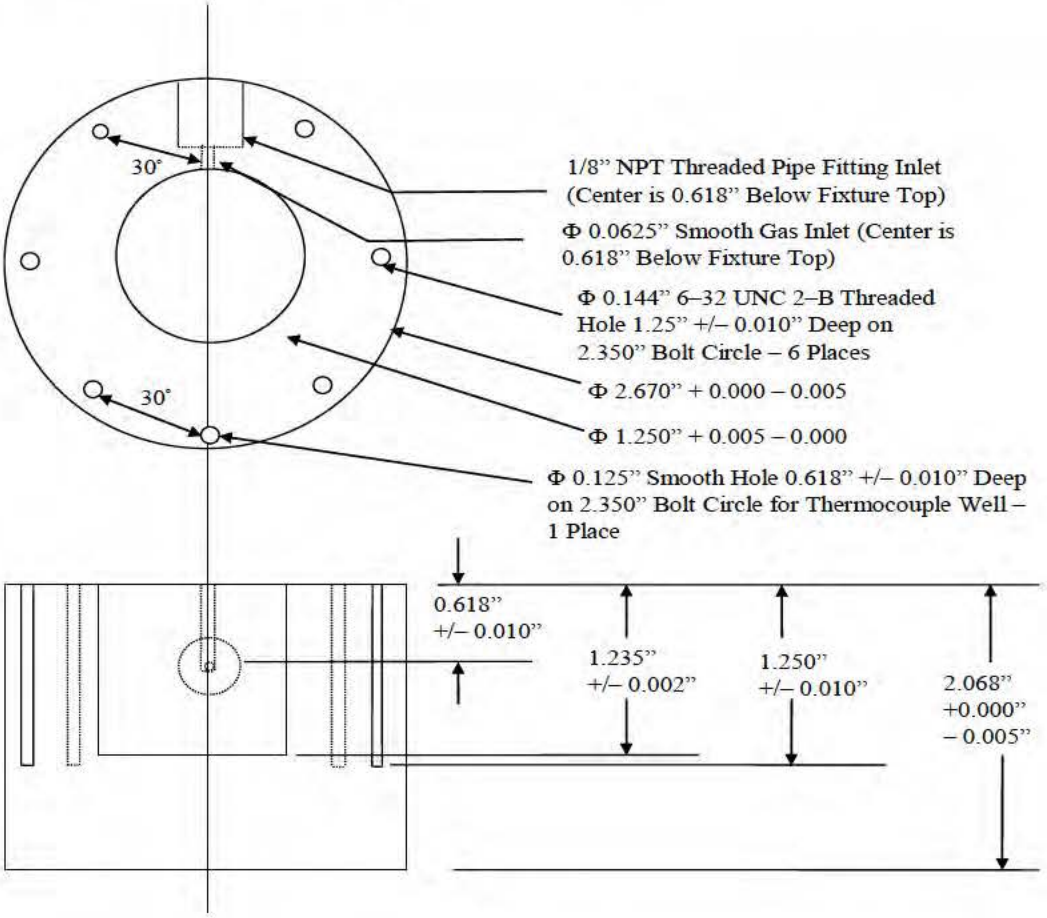

Fig. 28 Reusable SS test fixture (case)

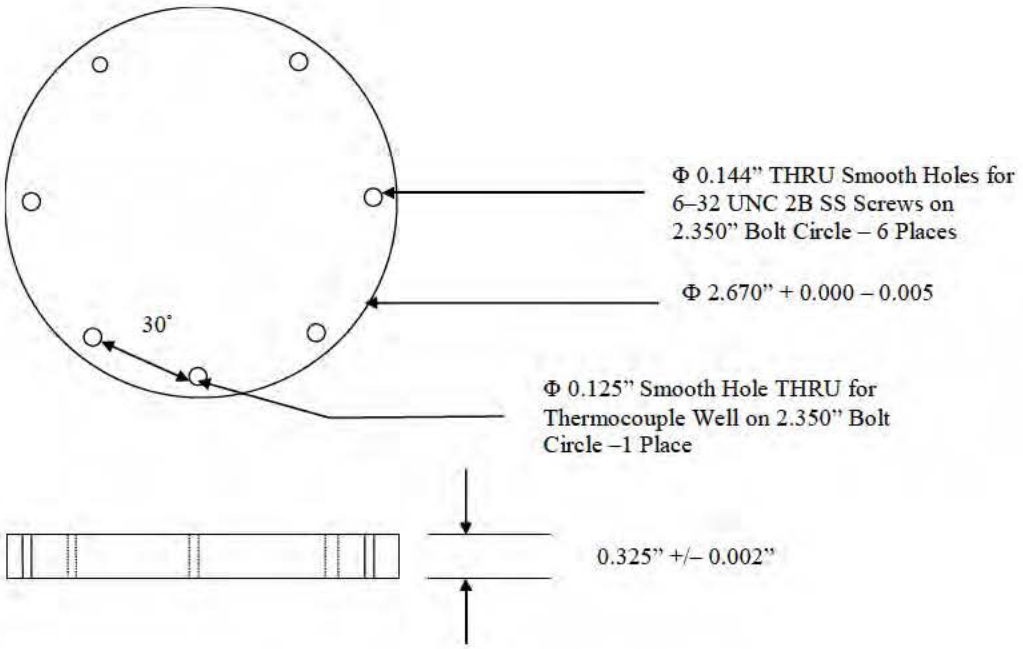

Fig. 29 Reusable SS test fixture (header)

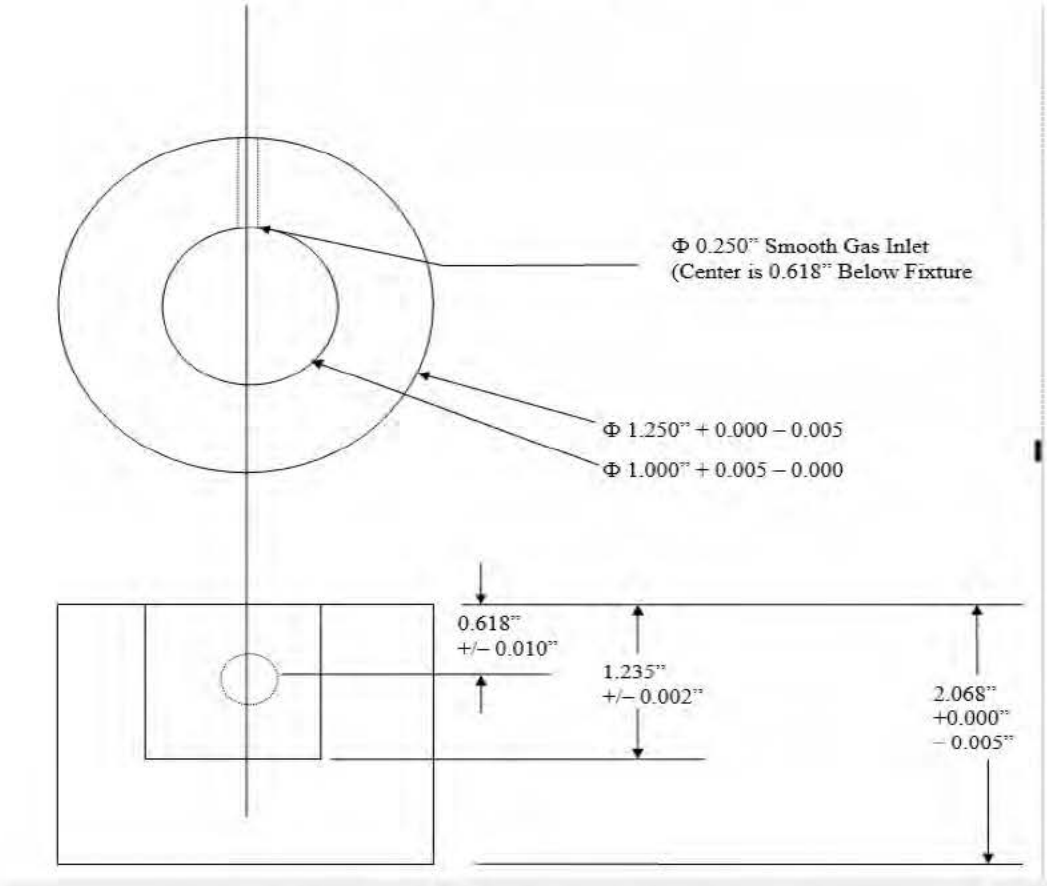

Fig. 30 Reusable SS test fixture (sample insert)

With the metal inserts (radial, axial, or both) it should be possible to build and test gas evolution and other parameters of interest for 3 or 4 simple laboratory type thermal batteries per day, rather than being limited to 1 battery test in 3 or 4 days as occurred previously when building complete, traditional, glass taped production style LCCM thermal cell stacks, and thermal insulation packages into laboratory test fixtures in anticipation of future LCCM flight tests. After testing the simply constructed thermal batteries and measuring the parameters of interest, the proposed new reusable test fixture can then be emptied and reused immediately. Externally the assembled laboratory test fixture will appear nearly identical to the previously reported reusable LCCM test fixture (see Fig. 26).

12. Summary and Conclusions

Pressed pellet thermal batteries presently used in missiles, artillery, and smart bombs as well as thin-film fast rise thermal batteries proposed for future small-arms and bunker penetration applications can both benefit from improved gas control methods, thermal modeling, and DOE statistical mathematical modeling analyses. Thermal models clearly show that pressed pellet thermal batteries can be markedly improved just by the removal of H_2 gas (lifetime extensions and energy density increases ranging from factors of 1.5 to 3). Significantly greater improvement is possible using previously reported enhanced gas control and thermal modeling methods.[1–11]

Previous gas evolution tests on thermal battery materials have shown that the oxidation of H_2 gas with $BaCrO_4$ to form H_2O is an effective and easily used method that might be used to remove H_2 from operating thermal battery atmospheres. Experimental evidence showed that the resulting H_2O vapor formed did not react with active thermal battery components to any measurable extent to form additional H_2 gas during battery operation ($2H_2O \leftrightarrow 2H_2 + O_2$). At higher battery case temperatures, more water vapor is ordinarily be present, but case temperatures have been measured as high as 200 °C during thermal battery operation without measurable formation of additional H_2 gas during battery operation. Evolved gases from pressed pellet thermal batteries tested during fiscal year 2015 (FY15) and before typically measured ~60–80 vol % H_2 gas initially and typically declined to ~50 vol % H_2 gas 300 to 500 s after battery initiation. For all pressed pellet thermal batteries tested to date, more than 94% of the evolved gases (excluding H_2O) consisted of H_2, O_2, N_2, CO, CH_4, and CO_2, where the gases are listed in the order that they eluted from the Carboxen 1010 GC PLOT Capillary Column used in the GC gas analyses.[1–5]

The cause for the failure to remove H_2 from the operating thermal battery using the heated Zr/$BaCrO_4$ ash reported here might be that the high $BaCrO_4$/heat paper powder weight ratio used in the battery tests described above ([0.5751] – or 6.01 g $BaCrO_4$ and 4.44 g of ~22/78 wt % Zr/$BaCrO_4$ paper powder) simply did not heat the $BaCrO_4$ sufficiently in the battery tests, or that the Zr/$BaCrO_4$ ash in the operating battery experiments was chemically altered from the ash formed in the previous gas evolution tests. The previous gas evolution tests[3] showed that a ratio of 0.3113 or 1.0950 g added $BaCrO_4$ and 2.4224 g of ~28/72 Zr/$BaCrO_4$ heat powder paper would remove 18.78 std-atm-cc of H_2 gas/g of added $BaCrO_4$. The 0.5751 ratio was determined by the preliminary battery electrical screening test results and was applied before the widely varying electrical lifetimes of the tested batteries became fully apparent as explained above.

A second possible reason for the failure to remove H_2 gas from the operating battery might be that the H_2 gas flowed too slowly from the thermal insulation package to react with the Zr/$BaCrO_4$ ash while the ash was still sufficiently hot. The second reason is intuitively attractive, but seems unlikely because calculations show that the thermal insulation package volume consists of mostly (~88%) void space. A third possible reason for difficulty might be that the Zr/$BaCrO_4$ weight ratio used was a borderline ratio that functions intermittently. A fourth possible reason for difficulty might be that excess CO, CO_2, and H_2O evolved when organic binders in the thermal insulation were heated reacted with the Zr/$BaCrO_4$ ash and made the ash incapable of removing the H_2 properly. It is also possible that overheating of the organic binder in the thermal insulation simply produced much more H_2 gas than was observed in the control battery and that the heated Zr/$BaCrO_4$ gas removed a great deal of this excess H_2 gas at or near previously observed H_2 gas removal rates.

The dip and recovery of the H_2 fraction in the operating gas atmosphere from 0 to 200 s in the battery with the heated Zr/$BaCrO_4$ ash shows that some H_2 was removed and that competing chemical reactions were present. As noted above in the introduction, materials selection and chemical processing methods to reduce the initial presence of chemically bound H_2 and H_2O content originally present in the battery materials should be pursued, but complete removal of H_2 gas in operating thermal batteries by materials selection and chemical processing alone seems unlikely because of the difficulty of completely removing chemically bound H_2 gas from materials like the pyrotechnic iron and because of the possibility of H_2O presence either in the hygroscopic electrolyte materials or adsorbed onto the porous thermal insulation materials. Water might also be reintroduced into even thoroughly dried thermal battery components as H_2O vapor during thermal battery construction.

The most likely cause for the present failure to remove H_2 gas seems to be the reaction of gas products from the overheated organic binder with the heated $Zr/BaCrO_4$ ash that rendered the ash incapable of removing significant amounts of H_2 gas. As noted above, the organic binder can easily be replaced with an inorganic binder used in an equivalent thermal insulation and the inorganic binder would not outgas significantly.

The available battery electrochemical capacity was only about 1/3 utilized, so that the batteries reported in the present tests were definitely heat limited. Lower H_2 gas fractions were produced than expected (about 60% by volume of the total gas mixture rather than about 80% by volume of the total gas mixture), but the effect of H_2 gas presence on measured thermal conductivity values should still be large. ARL Fortran and Sierra TABS analyses showed that thermal insulation package global thermal conductivity was lower than would be expected for the amount of H_2 gas that was found. The thermal cells might be generating more heat than allowed for in the model. Definitive tests of thermal cell stack heat generation would ultimately require individualized battery construction records with thermocouples attached to the thermal cell stack during discharge.

The method of removing H_2 gas using heated $Zr/BaCrO_4$ ash described here definitely shows promise and will be pursued further. As shown above, the control thermal battery evolved nominally 43.5 STP H_2 gas (or ~3.9 mg H_2) so that the amount of H_2 to be removed or eliminated from the starting materials is not large. Thermal conductivity measurements on a micro-porous thermal insulator has shown that if the H_2/air volume (mole) ratio can be held at or below 10/90, then the thermal conductivity of the micro-porous thermal insulator will be essentially as if only an air atmosphere were present in the porous structure and the desired thermal battery lifetime and energy density increases by factors of 1.5 to 3 mentioned above can still be achieved when using that micro-porous thermal insulator.

Effective implementation of such an easily applied method of H_2 gas control would make a great difference in the required volumes and available lifetimes of most present production thermal batteries. Uniformly smaller thermal batteries and uniformly more economical thermal insulation would become the new norm for the industry. Expensive micro-porous thermal insulators would not be required in many applications for which they are now essential.

After H_2 gas has been removed and thermal battery lifetimes and energy densities increased by factors of 1.5 to 3, thermal modeling shows that further significant improvements in thermal battery lifetimes and energy densities remain possible. These additional improvements would use some combination of enhanced gas control, thermal cell and thermal insulation package material choices, chemical

processing, and battery construction methods. Thermal modeling aided by DOE statistical analyses would help to choose the correct combination of parameters.

13. References

1. Krieger F, et al. Experimental and mathematical confirmation of munitions thermal battery heat transfer using FORTRAN and SIERRA finite element thermal models. Proc. 46th Power Sources Conference; 2014 July; p. 403.

2. Krieger F, Ding M. Gas analysis and control methods for thermal batteries. Adelphi (MD): Army Research Laboratory (US); 2013 Sep. Report No.: ARL-TR-6665.

3. Krieger F, Ding M. Thermal battery operating gas atmosphere control and heat transfer optimization. Adelphi (MD): Army Research Laboratory (US); 2012 Sep. Report No.: ARL-TR-6156.

4. Krieger F, et al. Gas control experiments and calculations for pressed pellet thermal batteries. Proc. 45th Power Sources Conference; 2012 June; p. 551.

5. Krieger F, Ding M. Heat transfer in the LCCM thermal reserve battery. Adelphi (MD): Army Research Laboratory (US); 2009 Sep. Report No.: ARL-TR-4843.

6. Ding M. et al. Developing nanofoil-heated thin-film thermal battery. Proc. 46th Power Sources Conference, 2014 July; p. 350.

7. Ding, M. et al. Developing nanofoil-heated thin-film thermal gattery. Adelphi (MD): Army Research Laboratory (US); 2013 Sep. Report No.: ARL-TR-6664.

8. Ding, M. et al Use of nanofoil as a new form of heat source in thermal batteries. Adelphi (MD): Army Research Laboratory (US); 2012 Sep. Report No.: ARL-TR-6141.

9. Piekos E, et al. Assessing the sensitivity of thermal battery performance to material thermal properties via simulation. Proc. 46th Power Sources Conference; 2014 July; p. 399.

10. Hewson J, et al. Model parameterization for electrochemical predictions of LiSi/FeS2 batteries. Proc. 46th Power Sources Conference; 2014 July; p. 407.

11. Roberts S, et al. Towards a coupled multiphysics model of molten salt battery mechanics. Proc. 46th Power Sources Conference; 2014 July; p. 411.

List of Symbols, Abbreviations, and Acronyms

ARDEC	Picatinny/Armament Research, Development, and Engineering Center
ARL	US Army Research Laboratory
$BaCrO_4$	barium chromate
CH_4	methane
CO	carbon monoxide
CO_2	carbon dioxide
DOE	design of experiment
FY15	fiscal year 2015
GC	gas chromatograph
GHS	gas handling system
H_2	hydrogen
H_2O	water
LCCM	Low Cost Competent Munition
N_2	nitrogen
NiAl	nickel aluminum
O_2	oxygen
PLOT	porous layer open tubular
SS	stainless steel
STP	standard temperature and pressure
TABS	Thermally Activated Battery Simulator
TIG	tungsten inert gas
UHP	ultra high purity
Zr	zirconium

1 DEFENSE TECH INFO CTR
(PDF) DTIC OCA

2 US ARMY RSRCH LAB
(PDF) IMAL HRA MAIL & RECORDS MGMT
RDRL CIO LL TECHL LIB

1 GOVT PRNTG OFC
(PDF) A MALHOTRA

6 US ARMY ARDEC
(PDF) AMSRD AAR MEF S
C MCMULLAN
RDAR EIF
C JANOW
RDAR MEF F
B ARMSTRONG
RDAR MEF F
M ALLENDE
K AMABILE
R DRATLER

3 SANDIA NATIONAL
(PDF) LABORATORIES
A GRILLET
D WESOLOWSKI
E PIEKOS

2 ADVANCED THERMAL
(PDF) BATTERIES, INC
D BRISCOE
G CHAGNON

3 EAGLE PICHER
(PDF) TECHNOLOGIES, LLC
C LAMB
J FERRARO
D BHAKTA

2 ENERSYS ADVANCED
(PDF) SYSTEMS
M STOKA
P SCHISSELBAUER

3 THE ENSER CORP
(PDF) D NIERMAN
R JACKSON
N SHUSTER

13 US ARMY RSRCH LAB
(PDF) RDRL SED C
M S DING
J MULLINS
C LUNDGREN
D BAKER
D TRAN
F KRIEGER
J READ
J SWANK
J WOLFENSTINE
RDRL SED E
I LEE
RDRL SED
E SHAFFER
RDRL SES S
A LADAS
RDRL SES X
J HOPKINS

INTENTIONALLY LEFT BLANK.